Photocatalytic degradation of Reactive Black 5 dye

Thesis submitted in partial fulfillment for the requirement of degree of

Master of Technology
in
Environmental Sciences and Technology

By:

SHUCHI

M. Tech. 2nd year

(Roll No. 601001027)

Under the guidance of

Dr. P. K. Bajpai
Distinguished Professor
Department of Chemical Engg.

Dr. Haripada Bhunia
Associate Professor
Department of Chemical Engg.

Department of Biotechnology and Environmental Science
THAPAR UNIVERSITY
Patiala, Punjab

June 2012

CERTIFICATE

This is to certify that the thesis entitled **"Photocatalytic degradation of Reactive Black 5 dye"**, is an authentic record of my own work carried out as requirements for the award of degree of Master of Technology in Environmental Science & Technology from Thapar University, Patiala, under the guidance of Dr. Pramod K. Bajpai (Distinguished Professor, ChED) and Dr. Haripada Bhunia (Associate Professor, ChED) during January to June 2012.

Shuchy

Shuchi
(Roll No: 601001027)

Date: 28/05/2012

It is certified that the above statement made by the student is correct to the best of our knowledge and belief.

Dr. P. K. Bajpai
Distinguished Professor
Department of Chemical Engineering
Thapar University, Patiala

Dr. Haripada Bhunia
Associate Professor
Department of Chemical Engineering
Thapar University, Patiala

Countersigned by:

Dr. M. S. Reddy
Head, Department of Biotech. & Env. Sciences
Thapar University, Patiala

Dr. S. K. Mohapatra
Dean of Academic Affairs
Thapar University, Patiala

ACKNOWLEDGEMENTS

I express my sincere gratitude and regards to my supervisor Dr. Pramod K. Bajpai, Distinguished Professor, Department of Chemical Engineering, Thapar University, Patiala for his valuable guidance and suggestions. Without his encouragement and guidance this thesis would not have been materialized.

I feel privileged to offer my sincere thanks and owe an enormous deal of gratitude to my co-supervisor Dr. Haripada Bhunia, Associate Professor, Department of Chemical Engineering, Thapar University Patiala, for his guidance and encouragement at every step of my work. He guided me and gave me full time to understand the minute details of each and every step, for the successful completion of my thesis work.

I would like to express my gratitude to Dr. M. S. Reddy, Head of department of Biotechnology and Environmental Sciences, Thapar University, Patiala for his kind cooperation and encouragement which helped in the completion of this work.

I would like to thank Dr. Rajeev Mehta, Head of Chemical Engineering Department, Thapar University, Patiala for supporting me and providing an environment to complete my work successfully.

I would like to thank my seniors Chitrakshi Goel and Kimi Jain, for their constant help and support at various stages of my thesis.

The generous support of all the staff members of Chemical Engineering Department is greatly appreciated

Above all, I express my indebtedness to the "**ALMIGHTY**" for all His blessing and kindness.

Shuchi
28/05/2012

Shuchi

(Roll No: 601001027)

ABSTRACT

The textile industries use a number of dyes, chemicals and other materials to impart desired quality to the fabrics. These industries generate a substantial quantity of effluents, the quality of which in most of the cases is unsuitable for further use and can cause environmental problems, if disposed off without proper treatment. At present, due to the increasing resource constraints and the environmental requirements, these textile industries need to adopt a sustainable approach, and wastes generated therefore to be viewed as unutilized resources. Ways and means must be found to recover water and chemicals from these "waste" resources. The conventional treatment processes have various disadvantages and limitations, therefore, cannot be successfully implemented in the textile industry. Advanced oxidation processes seem to be promising as these methods can efficiently degrade the highly toxic and recalcitrant compounds and do not generate any secondary pollutants for disposal.

Heterogeneous photocatalysis is the promising method among AOP's to remove colorants and also to completely degrade into simple substances like CO_2, H_2O and mineral acids. Various catalysts are used of which one of the most is studied TiO_2 due to its unique features such as absolute and relative band positions. The main disadvantage of using TiO_2 is the recombination of electrons and holes which can decrease the efficiency of the process which can be overcome by doping TiO_2 with metals and non metals.

This thesis seeks to give a method to study the kinetics of adsorption and of photocatalytic degradation of bare TiO_2 as well as doped TiO_2 which improves TiO_2 properties by doping with silver metal using liquid impregnation method. The dye used was Reactive black 5.

The **1st chapter** is an introduction, giving an overview of the situation and of the photocatalytic process as well as the literature review

The **2nd chapter** describes the materials and methods used during this research work.

The **3rd chapter** describes the kinetics of adsorption and of photocatalysis of undoped TiO_2.

The **4th chapter** describes the kinetics of adsorption and of photocatalysis of silver doped TiO_2.

CONTENTS

LIST OF FIGURES

LIST OF TABLES

ABBREVIATIONS

AOX	Adsorbable organic halogen
AOP	Advanced oxidation process
AR	Analytical reagent
BET	Branauer-Emmett-Teller
BOD	Biochemical oxygen demand
CB	Conduction band
COD	Chemical oxygen demand
e^-	Electron
ev	electron volt
g	gram
g/l	gram per litre
h^+	Hole
h	Plancks constant
l/mg	Litres per milligram
Ltd.	Limited
LI	Liquid impregnation
mg	Milligrams
mg/g	Milligrams per gram
mol	moles
nm	Nanometer
no.	Number
PEG	Polyethylene glycol
ppm	Parts per million
pvt.	Private
RPM	Revolutions per minute
RB 5	Reactive Black 5
TOC	Total organic carbon
UNESCO	United Nations Educational, Scientific and Cultural Organisation
UNICEF	United Nations Children's Fund
US	Ultrasound

UV	Ultraviolet
WHO	World Health Organization
VB	Valence band
Vis	Visible
ZPC	Zero point charge

CHEMICAL FORMULAE

TiO_2	Titanium dioxide
H_2O_2	Hydrogen peroxide
O_3	Ozone
$OH\bullet$	Hydroxyl radical
$O_2^{-}\bullet$	Superperoxide radical
CO_2	Carbon dioxide
H_2O	Water
$KMnO_4$	Potassium permanganate
O_2	Dioxygen
ZnO	Zinc oxide
WO_3	Tungsten oxide
MVO_4	Metal vanadates
In_2O_3	Indium oxide
CeO_2	Cerium oxide
$AgNO_3$	Silver nitrate
HCl	Hydrochloric acid
NaOH	Sodium hydroxide

CHAPTER 1

INTRODUCTION AND LITERATURE REVIEW

1.1 INTRODUCTION

Water is a pre-requisite for life and an adequate water supply in both quantity and quality is essential to human existence. Water covers three quarters of the earth surface but only 2.5 % is non salty. Over this 2.5 % world's fresh water less than 1 % is readily available for human use and is unevenly distributed (WHO, 2002).

World water consumption per year is about 10^4 km^3 and, at present, the quantity of available potential drinking water per year is between 10 and 30 x 10^3 km^3 (UNESCO, 2002). Therefore, even a small shortage of water could become a threat to mankind. It is estimated that (WHO, 2002; UNESCO, 2002;UNICEF, 2002):

(a) 2.2 million people in developing countries die every year from diseases associated with lack of safe drinking water

(b) 1.2 billions of people are lacking safe drinking water (one quarter of the world population)

(c) More than 80 countries are suffering from a lack of water (>40% of the world population).

Our biosphere is under constant threat from continuing environmental pollution. Impact on its atmosphere, hydrosphere and lithosphere by anthropogenic activities cannot be ignored. Man made activities on water by domestic, industrial, agriculture, shipping, radio-active, aquaculture wastes; on air by industrial pollutants, mobile combustion, burning of fuels, agricultural activities, ionization radiation, cosmic radiation, suspended particulate matter; and on land by domestic wastes, industrial waste, agricultural chemicals and fertilizers, acid rain, animal waste have negative influence over biotic and abiotic components on different natural eco-systems..

One of the most serious threats is the accumulation of non-biodegradable and toxic compounds in the ecosystem leading to the degradation of the quality of water sources and therefore of the drinking water.

Among many engineering disciplines, Textile Engineering has a direct connection with environmental aspects to be explicitly and abundantly considered. The main reason is that the textile industry plays an important role in the economy of the country like India and it accounts for around one third of total export. Out of various activities in textile industry, chemical processing contributes about 70% of pollution. Typical characteristics of textile effluent are shown in **Table 1.1**.

It is well known that cotton mills consume large volume of water for various processes such as sizing, desizing, scouring, bleaching, mercerization, dyeing, printing, finishing and ultimately washing. Due to the nature of various chemical processing of textiles, large volumes of waste water with numerous pollutants are discharged. Since these streams of water affect the aquatic eco-system in number of ways such as depleting the dissolved oxygen content or settlement of suspended substances in anaerobic condition, a special attention needs to be paid. Thus, a study on different measures which can be adopted to treat the waste water discharged from textile chemical processing industries to protect and safeguard our surroundings from possible pollution problem has been the focus point of many recent investigations. The Wastewater discharged from the textile industry is solution of complex chemical with high color value. The color in the effluent is mainly due to unfixed dye. The concentration of unused dyes in the effluent depends upon the nature of dyes and dyeing process underway at the time.

The treatments commonly used by the textile industries to treat their wastewaters are diverse. They are usually separated in preliminary, primary, secondary and tertiary stage. The preliminary treatment removes debris and sandy materials usually by a screening process. The primary treatment is the second step in separating undissolved materials. It separates suspended solids and greases from wastewater. The processes used in this treatment are physical: screening, sedimentation, flocculation, flotation. The secondary treatment is a biological treatment with micro-organisms. It is used to remove dissolved organic matter from the wastewater. The micro-organisms absorb organic matter from sewage as their food supply. The tertiary stage also called advanced wastewater treatment is usually used to achieve high quality effluent discharge. It

focuses on the removal of nutrient, phosphorus and solids. Dissolved solid removal for example can involve ion exchange, micro-porous membrane filtration, nano-filtration, reverse osmosis, adsorption and chemical oxidation (Peavy *et al*., 1985)

Table 1: Typical characteristics of textile effluent (Sahunin *et al*., 2006; Eswaramoorthi *et al*., 2008; Mehmet and Hasan 2002; Arslan *et al*., 2002; Bes-Pia *et al*., 2003; Aleboyeh *et al*., 2005; Metcalf and Eddy (2003))

pH	6.0-10.0
Temperature	35-45˚C
Biochemical Oxygen Demand (mg/l)	100-4,000
Chemical Oxygen Demand (mg/l)	150-10,000
Total Suspended Solids (mg/l)	100-5000
Total Dissolved Solids (mg/l)	1,800-6,000
Chlorides (mg/l)	1,000-6,000
Total Alkanity (mg/l)	500-800
Sodium (mg/l)	600-2,175
Total Kjeldahl Nitrogen (mg/l)	70-80
Color (Pt-Co units)	50-2,500

Nevertheless these treatments might not be sufficient to remove all toxic compounds. For example, some of these treatments (reverse osmosis, nano-filtration, etc.) only transfer the pollutant matter from the aqueous phase to a second one but do not destroy it. The non-biodegradable compounds are usually very hard to degrade and are decreasing the efficiency of the secondary stage. Some contaminants can also be toxic to the bio-culture of the secondary stage. Moreover, they have tendency to contaminate food chains through bioaccumulation phenomenon. The latest developments in the decontamination of water is to improve the elimination rate of those bio-recalcitrant molecules.

In the last decade, a lot of research has been addressed to a particular class of oxidation process called Advanced Oxidation Process (AOP). It has been shown that AOP could be highly efficient to mineralize non-biodegradable molecules into relatively non-toxic inorganic ions and further into CO_2, H_2O and mineral acids at ambient temperature and atmospheric pressure. This process could considerably reduce the AOX quantity as well as the toxicity of the effluent making it easier for the mills to meet the imposed requirements. One of its drawbacks is its relatively high operational cost. However, this process could come as a pretreatment before the secondary stage (**Fig. 1.1**), therefore solving the problem of the loss of efficiency of the secondary treatment and be economically viable.

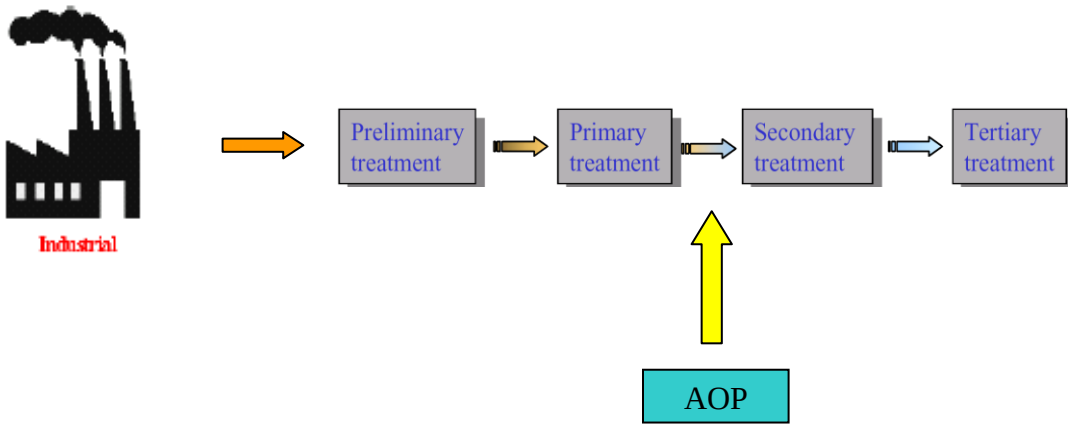

Fig. 1.1 Schematic representation of wastewater treatment

Three AOPs have emerged in the last few years, the photocatalytic process, the sonolysis and the radiolysis gamma.

It is possible to classify the different AOPs (**Fig. 1.2**). The first parameter is the reaction phase. Indeed either only wet chemical are used, leading to a homogeneous medium or a catalyst in a solid form is used leading to a heterogeneous medium. The second parameter is the nature of the external energy and the third is the way the OH● are produced. The strong potential for water purification of the photocatalytic process is widely recognized but due to high energy cost as

Classification			Process
Reaction Phase	External Energy	Generation of Hydroxyl radicals	
Homogeneous	Light	Photochemical Process / Chemical Process	UV/O_3
			UV/H_2O_2
			$UV/H_2O_2/O_3$
			$UV/F^{2+}(Fe^{3+})/H_2O_2$
	Light /Ultrasound	Photochemical/ Sonochemical process	UV/US
	Ultrasound	Sonochemical process	US/H_2O_2
			US/O_3
	High-energy electrons	Ionising radiation process	Electron Beam
	None	Chemical process	H_2O_2/O_3
	None	Chemical process	O_3/H_2O_2/high pH
	None	Chemical process	F^{2+}/H_2O_2(Fenton)
	None	Electrochemical/ Chemical process	Electro-Fenton
Heterogeneous	Light	Photochemical process	$UV/TiO_2/O_2$
			$UV/TiO_2/H_2O_2$
	None	Chemical process	Iron Oxide/H_2O_2

Fig. 1.2 Advanced Oxidation Processes (Poyatas *et al*., 2010)

is the generation of free hydroxyl radical (OH●), a highly reactive, non-selective oxidizing agent (EH=2.8 V), which can destroy even the recalcitrant pollutants. Hydroxyl radicals (HO•) are effective in destroying organic chemicals because they are reactive electrophiles (electron preferring) that react rapidly and nonselectively with nearly all electron-rich organic compounds exhibit faster rates of oxidation reactions comparing to conventional oxidants such as H_2O_2 or $KMnO_4$. Once generated, the hydroxyl radicals can attack organic chemicals by radical addition (Eq. (1)), hydrogen abstraction (Eq. (2)) and electron transfer (Eq. (3)) (SES, 1994). In the following reactions, R is used to describe the reacting organic compound.

$$R + HO\bullet \rightarrow ROH \quad (1)$$

$$R + HO\bullet \rightarrow R\bullet + H_2O \quad (2)$$

$$R^n + HO\bullet \rightarrow R^{n-1} + OH^- \quad (3)$$

Heterogeneous advanced oxidation processes generally use catalysts to carry out the degradation of compounds. In comparison to homogeneous processes, such heterogeneous catalysts have the advantage of separating the product with greater ease. For industrial applications, these catalysts should have certain characteristics such as: (1) high activity; (2) resistance to poisoning and long-term stability at high temperatures; (3) mechanical stability and resistance to attrition; (4) non-selectivity in most cases; and (5) physical and chemical stability under a wide range of conditions. Catalysts can be classified as metal catalysts, metal oxide catalysts and organo- metal catalyst. Heterogeneous photocatalysis is the type of heterogeneous AOPs most commonly used these days.

1.2 LITERATURE REVIEW

1.2.1 Generalities

New processes are to be developed to better treat effluents coming from polluting industries. It has been found that advanced oxidation process (AOP) is highly efficient to mineralize non-biodegradable molecules into relatively non- toxic inorganic ions and further into CO_2, H_2O and mineral acids. Different AOP's exist, but the one that seems relatively interesting is a photo-catalytic process with TiO_2 as catalyst. It has been reported in numerous articles that the heterogeneous process using TiO_2 as catalyst is efficient to oxidize organic compounds such as chlorinated phenols, dyes and others like pesticides (Toor, 2005; Toor *et al*., 2006; Al-Bastaki, 2003; Muruganandham *et al*., 2007). The versatility of AOP's is also enhanced by the fact that they offer different possible ways for hydroxyl radical production and thus allowing a better compliance with the specific treatment requirements (Muruganandham *et al*., 2007)

In 1972, Fujishima and Honda discovered the photocatalytic splitting of water on TiO_2 e1ectrodes. This event marked the beginning of a new era in heterogeneous photocatalysis. Since then research efforts in understanding the fundamental processes and in enhancing the photocatalytic efficiency of TiO_2 have come from extensive research performed by chemists, physicists and chemical engineers. Such studies are often related to energy renewal and energy

storage. In recent years, applications to environmental cleanup have been one of the most active areas in heterogeneous photocatalysis. This is inspired by the potential application of TiO_2-based photocatalysts for the total destruction of organic compounds in polluted air and wastewater.

In a heterogeneous photocatalysis system, photoinduced molecular transformations or reactions take place at the surface of a catalyst. Depending on where the initial excitation occurs, photocatalysis can be generally divided into two classes of processes. When the initial photoexcitation occurs in an adsorbate molecule which then interacts with the ground state catalyst substrate, the process is referred to as a catalyzed photoreaction. When the initial photo excitation takes place in the catalyst substrate and the photoexcited catalyst then transfers an electron or energy into a ground state molecule, the process is referred to as a sensitized photoreaction. The initial excitation of the system is followed by subsequent electron transfer and/or energy transfer. It is the subsequent deexcitation processes (via electron transfer or energy transfer) that leads to chemical reactions in the heterogeneous photocatalysis process.

1.2.2 Theory

The photo-catalytic process is based on the irradiation of a catalyst, usually a semi-conductor that creates electron donor and acceptor sites allowing the formation of a highly oxidizing agent: $OH^{\bullet}$. This powerful reactive species attacks with a relatively high rate of reaction and non-selectively most of the organic molecules (Hoffman *et al*., 1994)

When a semi-conductor gets photo excited, the electrons that are in the valence band can get promoted to the conduction band if the energy brought by the light is higher than that of the band gap. (The band gap is the gap between the valence band and the conductor band i.e. the highest occupied and the lowest unoccupied energy bands. To cross this region, devoid of energy levels, an electron has to get as much energy as the difference of energy between the conduction band and the valence band).

This promotion leads to a hole (h^+) in the conduction band, that will rapidly be trapped inside the particle to create an electron acceptor site, and to an electron in the valence band that will also be trapped offering therefore an electron donor site.

It is important to notice that recombination, with release of heat, can occur on a nanosecond time scale.

The most commonly accepted theory is the following one (**Fig. 1.3**)

$TiO_2 \longrightarrow TiO_2 + h^+ + e^-$ (4)

$H_2O_{ads} + h^+ \longrightarrow h^+ + OH_{ads}\bullet$ (5)

$OH_{ads}^- + h_{VB}^+ \longrightarrow OH_{ads}\bullet$ (6)

$O_2 + e^- \longrightarrow O_2\bullet$ (7)

$H_2O_2 + O_2\bullet \longrightarrow O_2 + OH^- + OH\bullet$ (8)

Recombination

$TiO_2 + h_{VB}^+ + e_{CB}^- \longrightarrow TiO_2 + heat$ (9)

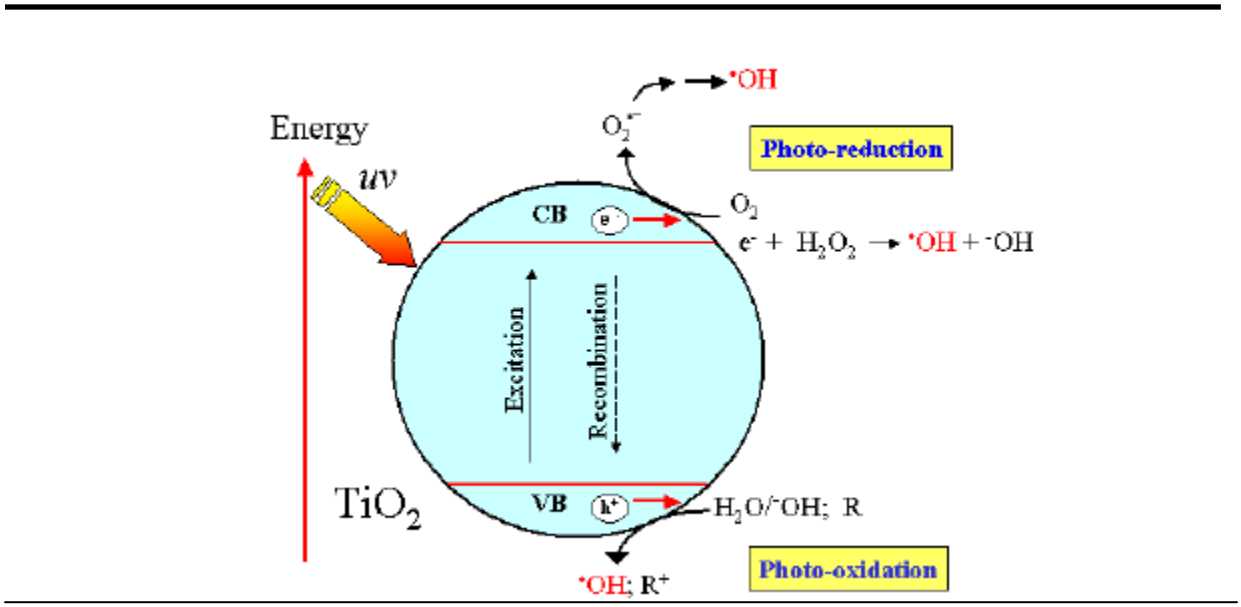

Fig. 1.3 TiO_2-semiconductor photocatalytic process. Scheme showing some photochemical and photophysical events that might take place on an irradiated semiconductor particle (Galvez and Rodriguez, 2003).

The hydroxyl radicals are produced by the oxidation of water on an electron acceptor site or by the reduction of oxygen on a electron donor site giving $O_2^{\bullet -}$ that reacts with water to form hydrogen peroxide that get further reduced on another electron donor site, finally giving the hydroxyl radical.

The kinetic for this kind has been studied and follows Langmuir and Freundlich isotherms.

The equation corresponding to the pseudo-first order kinetic model is the following:

$$log\frac{q_e}{q_e-q_t} = \frac{k_1}{2.303}t \quad (10)$$

where q_e and q_t refer to the amount of dye adsorbed (mg/g) at equilibrium and at any time, t (min), respectively, and k_1 is the equilibrium rate constant of the pseudo-first sorption (1/min). Eq. (10) can be arranged to obtain a linear form

$$\log(q_e - q_t) = \log q_e - \frac{k_1}{2.303}t \quad (11)$$

The equation corresponding to the pseudo-second-order kinetic model is the following

$$\frac{1}{q_e - q_t} = \frac{1}{q_e} + k_2 t \quad (12)$$

Where k_2 is the equilibrium rate constant of the pseudo-second-order adsorption (g/mg/min). Eq. (12) can be arranged to obtain linear form:

$$\frac{t}{q_t} = \frac{1}{k_2 q_e^2} + \frac{1}{q_e}t \quad (13)$$

The theoretical langmuir isotherm equation can be represented as

$$q_e = \frac{q_{mon} K_L C_e}{1 + K_L C_e} \quad (14)$$

Where K_L is the langmuir constant related to the energy of adsorption (l/mg) and q_{mon} is the maximum amount of adsorption corresponding to complete monolayer coverage on the surface (mg/g). The constants K_L and q_{mon} can be determined from the following linearised form

$$\frac{C_e}{q_e} = \frac{C_e}{q_{mon}} + \frac{1}{K_L\ q_{mon}} \quad (15)$$

The essential feautures of Langmuir adsorption isotherm can be expressed in terms of a dimensionless constant called the separation factor or equilibrium parameter (R_L). Conformation

of the experimental data into Langmuir isotherm model indicates the homogeneous nature of the catalyst surface.

$$R_L = \frac{1}{1+K_L C_0} \quad (16)$$

The Freundlich isotherm can be used for non-ideal sorption that involves heterogeneous surface energy systems and is expressed by the following equation:

$$q_e = K_F C_e^{1/n} \quad (17)$$

Where K_F is a rough indicator of the adsorption capacity and 1/n is the adsorption intensity. In general, as the K_F value increases the adsorption capacity of an adsorbent for a given adsorbate increases. Eq. (17) may be linearised by taking logarithms:

$$log q_e = log K_F + \frac{1}{n} log C_e \quad (18)$$

Conformation of the experimental data into Freundlich isotherm indicates the heterogeneous nature of the TiO_2 surface.

The processes of degradation for heterogeneous photocatalysis include (i) mass transfer (from the medium to the catalyst), (ii) diffusion, (iii) adsorption, (iv) competition at the surface of the catalyst between the different species, (v) the mechanistic events that take place before any reaction to produce electron-hole pairs from the energy provided by the light.

Several mechanisms can lead to the degradation of the pollutant. There could be adsorption of the pollutant at the surface of the catalyst as well as adsorption of O_2, H_2O, etc. and the reaction could take place at the surface. The hydroxyl radicals could be adsorbed at the surface and the pollutant reacts with it, being in the bulk solution. The pollutant could be absorbed and the hydroxyl radicals in the solution and finally, the pollutant and the hydroxyl radicals could be both in solution.

The photocatalytic degradation of organic pollutants in water generally follows a Langmuir–Hinshelwood mechanism (Turchi *et al*., 1990; Al-Sayyed *et al*., 1991), with the rate being proportional to the coverage θ

$$r = -\frac{dC}{dt} = k\theta = k\frac{K_{ads}C}{1+K_{ads}C} \quad (19)$$

where *k* is the true rate constant which is dependent upon various parameters such as the mass of catalyst, the flux of efficient photons, the coverage in oxygen, etc., K_{ads} the adsorption constant, *t* the time and *C* is the concentration of organic pollutant. The product of K_{ads} and initial concentration cannot be neglected with respect to 1 in the denominator of r at higher concentrations. Eq. (19) can be rearranged as

$$\frac{1}{k_{app}} = \frac{C_o}{k} + \frac{1}{k\,K_{ads}} \quad (20)$$

The photocatalytic oxidation rate approaches first order:

$$r = -\frac{dC}{dt} = kK_{ads}C = k'C \quad (21)$$

where *k*' is the apparent rate constant of the pseudo-first order kinetics. The integral form, *C*= *f*(*t*) of the rate equation is:

$$-ln\frac{C}{C_O} = k_{app}t \quad (22)$$

where C_O is the initial concentration of pollutant

For the study of adsorption thermodynamics, experiment was conducted at 298 K temperature in order to determine standard free energy (ΔG^o). The Gibbs free energy of the adsorption process is related to the equilibrium constant by Eq. (23).

$$\Delta G° = -RT \ln K \quad (23)$$

Where R (8.314 J/mol.K) is the gas constant, T (K) the absolute temperature and K (l/g) is the standard thermodynamic equilibrium constant defined by q_e/C_e.

1.2.3 Heterogeneous photocatalysts

Unlike metals, which have a continuum of electronic states, semiconductors exhibit a void energy region in which no energy levels are available to promote the recombination of an electron and hole produced by photoactivation in the solid. The void region that extends from the top of the filled valence band to the bottom of the vacant conduction band is called the band gap (Linsbigler *et al*., 1995)

Absorption of a photon by semiconducting solids excites an electron (e^-) from the valence band to the conduction band if the photon energy, $h\upsilon$, equals or exceeds the band gap of the semiconductor/photocatalyst. Simultaneously, an electron vacancy or a positive charge called a hole (h^+) is also generated in the valence band. Ultraviolet (UV) or near-ultraviolet photons are typically required for this kind of reaction. The electron-hole pair (e^-h^+ pair) thus created migrates to the photocatalyst surface where it either recombines, producing thermal energy, or participates in redox reactions with the compounds adsorbed on the photocatalyst. The life time of an e^-h^+ pair is a few nanoseconds (but this is still long enough for promoting redox reactions in the solution or gas phase in contact with the semiconductor.

Semiconductor photocatalysts are preferred in photocatalytic treatments of dye waste-water for the following reasons: (i) they are inexpensive; (ii) they contain low to no toxicity; (iii) they exhibit tunable properties that can be modified such as by size reduction, doping, or sensitizers; (iv) they contain an affording facility for a multielectron transfer process; and (v) they are capable of extending their use without substantial loss in photocatalytic activity (Chattergee *et al.*, 2005).

Several metal oxides have been reported to be good photocatalysts, namely titanium dioxide (TiO_2), zinc oxide (ZnO), tungstate (WO_3), vanadate (VO_4), molybdate (MoO_4) and others (Chakrabarti *et al*., 2004; Janitabar-Darzi *et al*., 2004; Guo *et al*., 2010). The photocatalytic properties of these metal oxides have been studied extensively and results show that they have active potential as photocatalysts in the degradation of dye in wastewater.

Metal oxides photocatalysts such as zinc, vanadium, tungsten, molybdenum, iridium and cerium oxides have been used to treat dye waste water. Some studies showed that these photocatalysts could be as effective or even better than conventional photocatalysts.

The quantum efficiency of ZnO is significantly larger than that of TiO_2. Thus, ZnO absorbs over a larger fraction of the solar spectrum rendering it a more suitable photocatalyst for use under visible light conditions (Chakrabarti *et al*., 2005; Qiu *et al*., 2007; Behnajady *et al*., 2009). Some of the most recent experimental results also showed that ZnO actually exhibits a higher photocatalytic activity than TiO_2 especially when the degradation of industrial effluents occurs at neutral pH. ZnO showed promising results as a photocatalyst for the degradation of azo dyes (Orange II and Direct Yellow 12) and some reactive dyes (Remazol Black B and Remazol Brilliant Blue R) (Gouvea et al., 2000) under UV conditions. For example, Nishio *et al*. (2006) and Gouvˆea *et al.* (2010) found that using ZnO the model dye could be completely bleached by 60 min of UV light irradiation. Also, high TOC removal of Remazol Brilliant Blue R (up to 90%) could be achieved using ZnO with 120 min of UV light irradiation. Although ZnO (3.2 eV) has a wide band gap, it has better quantum efficiency than TiO_2 makes it a better photocatalyst with solar irradiation. Lu *et al*. (2009) and Mai *et al*. (2008) utilized ZnO nanoparticles (50–70 nm; BET surface area: 15–25 m^2/g) in the degradation of triphenylmethane dyes (BB-11) and Methyl Green respectively. Both found that complete degradation of dye was achieved after 20 h reaction. However Pare *et al*. (2008) found that if higher intensity (500 W) visible light was used, complete degradation and COD reduction of Acridine Orange could be obtained after only 3 h irradiation using ZnO powder. Kansal *et al*. (2007) compared the photocatalytic efficiency of different semiconductors (ZnO, TiO_2, SnO_2, CdS and ZnS) on dye degradation under UV and solar light irradiation. They reported that ZnO (under both irradiation conditions) was the most active photocatalyst for decolorization of Methyl Orange and Rhodamine 6G. Furthermore, the decolorization of both dyes occurred at a faster rate using solar radiation compared with UV light. Their results implied that ZnO can harvest maximum solar energy by utilizing visible light for degradation of water bound organics.

Metal vanadates (MVO_4) have recently been considered as potential semiconductors in dye waste-water treatment. Recently, the main focus has been on the development of bismuth

vanadate ($BiVO_4$) which has been reported to be active in the degradation of dye wastewater under visible light irradiation. Bismuth vanadate is a typical ternary semiconductor compound with a layered structure (band gap ca 2.4 eV), which exists mainly in three crystal structures: tetragonal scheelite (ts), monoclinic scheelite (ms) and tetragonal zircon (tz). Among these crystalline phases, ms-$BiVO_4$ exhibits a higher photocatalytic activity than either ts- or tz-$BiVO_4$. Shang *et al*. (2009) reported that nanosized $BiVO_4$ (ca 60 nm) with strong visible light induced photocatalytic activity could be synthesized under ultrasonic irradiation using polyethylene glycol (PEG) as a stabilizing agent. They found that the nanosized $BiVO_4$ exhibited excellent visible light driven photocatalytic efficiency for degrading Rhodamine B; with 1.0 g PEG-modified $BiVO_4$ fully degrading Rhodamine B in 40 min and reducing the COD content by up to 72.7% in 3.5 h. In contrast, the degradation rate of non-PEG modified $BiVO_4$ (183 nm) reached 28% after 40 min of visible light irradiation. Thus, the nanosized $BiVO_4$ by possessing a large surface area, an appropriate band gap and a small crystal size enhances the photocatalytic activity in visible light by up to 12 times higher than catalysts prepared by the traditional solid state reaction.

Tungsten oxide (WO_3) was also reported to be photocatalytically active and effective for the treatment of dye wastewater. According to Cruz *et al*. (2010) the different morphologies and physical properties of WO_3, such as the band gap energy and surface area would determine the treatment efficiency. For example, samples with square-plate morphologies and higher surface areas showed the highest TOC reduction of Indigo Carmine (up to 93% within 75 h), which performed better than the commercial catalyst Degussa P25. However, complete mineralization of Rhodamine B and Congo Red by WO_3 photocatalyst was not as feasible as using Degussa P25. The results indicated that WO_3 is not a very versatile photocatalyst compared with TiO_2 but in the treatment of a particular dye in wastewater the WO_3 still proves to be a useful catalyst. Further studies should be conducted to assess its photocatalytic potential.

In recent years, indium oxide (In_2O_3) which can absorb light wavelength <480 nm and has a band gap of about 2.5 eV, has been studied extensively in efforts to obtain high photocatalytic activity and has been used to produce many single phased multicomponent oxides (Tang *et al*., 2004; Ding *et al*., 2009) or used as doping agent for TiO_2 (Yang *et al*., 2008). For example Tang

et al. (2004) using a solid state reaction, synthesized a series of MIn_2O_4 (M = Ca,Sr,Ba) photocatalysts which exhibited higher activity for Methylene Blue photodegradation under visible light than commercial Degussa P25, especially when $CaIn_2O_4$ was used as photocatalyst. From calculation of the band structure, they found that the smaller the radii of the M ion, the stronger the oxidative ability of the valance band of the oxide. However, by using the solid state reaction, evaporation of In_2O_3 above 1273 K made the process of synthesizing pure $CaIn_2O_4$ phase difficult. Ding *et al*. (2009) reported a new method of synthesis at a relatively low temperature (lowest temperature 473 K) using solution-combustion of calcium nitrate and indium nitrate as oxidizers and glycine as a fuel, followed by high temperature post annealing (1373 K). Remarkably, this method produced $CaIn_2O_4$ rods which showed higher photocatalytic activity for Methylene Blue degradation under visible light irradiation than $CaIn_2O_4$ synthesized by the solid state reaction. The $CaIn_2O_4$ rods took only 90 min to decompose Methylene Blue under visible light irradiation.

According to Hern´andez-Alonso *et al*. 2009 cerium oxide (CeO_2) has received attention as a photocatalyst because of its unique properties of stability under illumination and strong absorption for both UV and visible light. Pure nanocrystalline cubic phase CeO_2 can be prepared using cerium nitrate, NH_4HCO_3 and polyethylene glycol 1000 as raw material, precipitant and dispersant, respectively. Under appropriate conditions, the synthesized nanocrystalline CeO_2 was able to degrade Acidic Black 10B up to 97% using sunlight irradiation. Viana *et al*. (2009) reported the possibility of synthesizing Ce ion-exchanged titanate nanotubes (Ce–TiNTs) and their potential as a photocatalyst under natural sunlight. They found that the Ce–TiNTs could reduce the colour of Reactive Blue 19 to about 30% in 50 min in sunlight.

TiO_2 has a band gap of 3.2 eV. meaning that electrons can get promoted if they are excited by light with a wavelength of 387 nm or under, i.e. the near UV portion of the solar radiation which forms about 5% of the total spectrum. It is, therefore possible to use this catalyst under sun light conditions. Its conductance band's potential is 3.1 eV, which is enough to oxidize molecular oxygen and peroxide to give hydroxyl radicals. The valence band's potential is -0.1 eV. which allows to reduce water and OH^- to form hydroxyl radicals. In other terms, the redox potentials of $H_2O/OH^{\bullet}$ $O_2/O_2^{\bullet}$, $H_2O_2/OH^{\bullet}$ couples lie within the band gap of TiO_2 (**Fig. 1.4**). Moreover, TiO_2

is photo-stable, insoluble, non-toxic, biologically and chemically inert and available at relatively modest price. It could also be recycled on a technical scale. TiO_2 has proven to be a suitable catalyst for widespread environmental applications (Taylor & Francis, 2005). TiO_2 and more specifically, Degussa P25 in the anatase, form has been chosen as a reference in most of the literature. Indeed it has proven to be an excellent catalyst (its photocatalytic activity is substantially higher than most of the other readily available samples) and its structural properties are well known. Usually it has a non porous structure with 70%/30% anatase-to-rutile mixture. Its BET surface area is about 55 ± 15 m^2/g and crystallite sizes of 30 nm in 0.1 diameter aggregates.

To summarize, the reason for TiO_2's widespread use comes from its moderate band gap, nontoxicity, high surface area, low cost, recyclability, high photoactivity, wide range of processing procedures, and its excellent chemical and photochemical stability, as well as its availability. TiO_2 is ranked in the 50 more available chemicals on earth.) (Wade, 2005).

TiO_2 is the preferred catalyst for the photocatalytic treatment of dye wastewater. TiO_2 is used as a photocatalyst in dye wastewater treatment mainly because of its ability to generate a high oxidizing electron–hole pair, its good chemical stability, non-toxicity and long-term photostability (Han *et al*., 2009; Chaterjee *et al*., 2005; Zhang and Song, 2009). TiO_2 naturally occurs in three common crystalline polymorphs: anatase, rutile and brookite. Although the anatase phase is considered the most photocatalytically active phase, rutile is the most thermodynamically stable and is about 1.2–2.8 kcal/mol more stable than anatase (Zheng *et al*., 2010). Also, the wide energy band gap (e_g > 3.2 eV) in anatase may limit its potential because only UV light with wavelengths less than 387 nm can initiate the electron–hole separation process. Consequently, it is a great challenge to tailor a good photocatalyst from TiO_2 that can efficiently harness the energy from natural sunlight, which consists of no more than 5% UV light and 45% visible light.

Up to now, several modifications of the structure of TiO_2 have been made to achieve the following: (i) reduce the band gap energy to a solar light-compatible level (ii) enhance the efficiency of electron–hole production; and (iii) enhance the absorbency of organic pollutants

onto TiO_2 by modifying the surface structure. The structure of TiO_2 can be modified by doping with certain metal ions, such as rare earth metals, noble metals and transition metals as well as non-metals such as C, N, S and P (Zheng *at al*., 2010; Zhang and Song, 2009; Lv *et al*., 2009; Znad *et al*., 2009; Janus *et al*., 2009)

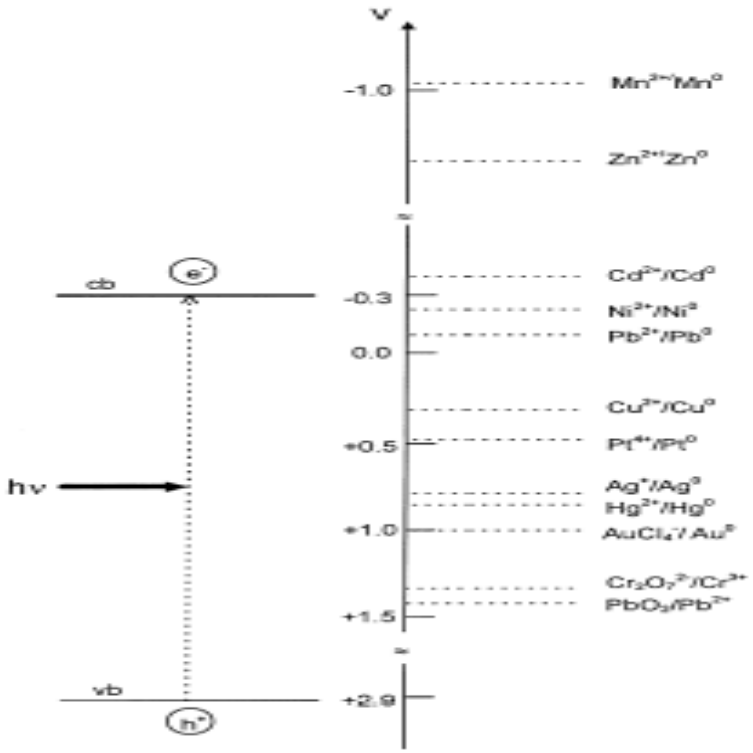

Fig. 1.4 Red-ox potential of TiO_2 (Galvez and Rodriguez, 2003).

Noble metals (Au, Pt, Ag and Pd) are usually used as dopants to modify the TiO_2 structure. However, recently transition metals (Cr, Mn, Fe, Co, Ni, Cu and Zn) have been used to replace noble metals and thus, to reduce the overall catalyst production cost. Ghasemi *et al*. (2009) found that TiO_2-doped Fe gave the best results, with more than 90% degradation and 75% TOC removal efficiency of Acid Blue 92 upon UV light irradiation. The incorporation of transition metal ions into the TiO_2 lattice was found to alter or lower the band gap energy and shift the catalyst absorbance edge closer to the visible light region.

El-Bahy *et al*. (2009) and Zhu *et al*. (2010) took this step further by synthesizing TiO_2 with a sol–gel method and, at the same time incorporating RE metal ions into the catalyst structure. The synthesized TiO_2 with the addition of the RE ions (La^{3+}, Nd^{3+}, Sm^{3+}, Eu^{3+}, Gd^{3+} or Yb^{3+}) produced RE-doped TiO_2 with Gd-TiO_2, which exhibited the highest decolorization (91.5%) of Direct Blue Dye (DB53) under UV irradiation. Zhu *et al*. (2010) reported that the decolorizing efficiency of 91.2% for Methylene Blue after 180 min irradiation with sunlight using Ce^{3+}-doped TiO_2-SiO_2.

Generally, there is growing concern over the recovery of TiO_2 from the reactor if the AOP process is scaled up for industrial application. According to Pozzo *et al*. (1997) although TiO_2 is an effective catalyst in dye waste-water treatment, the post treatment to separate the catalyst from treated water is difficult and not cost effective. In addition, TiO_2 particles dispersed in the aqueous solution tend to coagulate in a prolonged photocatalytic degradation process, causing reduction of both the surface area and treatment efficiency. In most bench-scale studies, catalysts are often separated by simple centrifugation or filtration. However, this is not feasible for separating catalyst at an industrial scale, mainly due to the energy and time consumed by the separation processes. Consequently, research on the immobilization or synthesis of TiO_2 particles with magnetic behaviour is gaining importance. TiO_2 particles were also synthesized by coating a TiO_2 precursor onto the surface of a ferromagnetic particle, acting as a magnetic core. Several magnetic TiO_2 specieswere reported, from simple maghemite (γ -Fe_3O_4) coated with TiO_2 to a mixture of silica (SiO_2) and titania (TiO_2) coatings on magnetite iron oxide (Fe_3O_4) (Gao *et al*., 2003). These magnetic TiO_2 species can easily be separated from treated wastewater using a magnetic field. Furthermore, this new type of photocatalyst usually exhibits high photocatalytic efficiency; for example, Kurinobu *et al*. (1999) found that TiO_2 and SiO_2 coated on a Fe_3O_4 magnetic core could completely degrade three different types of dyes in 240 min under UV irradiation.

1.2.4 Modified TiO_2

The TiO_2 has two main problems (a) high energy requirements (photo response). Value of band gap is 3.2ev hence it can absorb wavelength less than 388 nm in UV light spectrum therefore TiO_2 can absorb only 2-3% of solar energies. Due to this reason natural light can’t be used for

photo catalysis. (b) The main disadvantage of using TiO_2 is the recombination of electrons and holes (Eq. (9)) which can decrease the efficiency of the process.

$$TiO_2 (e^- + h^+) \longrightarrow TiO_2 + \text{heat} \quad (9)$$

Various attempts have been made to increase the photo catalytic activity of TiO_2 which includes modifying the various properties of TiO_2. Modifying the electronic and optical properties of TiO_2 include incorporating impurities, doping or band-gap engineering principles. The band gap can be modified through various strategies such as mixing conduction-band states with lower levels, thus lifting the valence band (for example N incorporation and possibly C doping). Modification of the optical and electrical properties can also involve introducing new energy bands or localized states in the band gap of TiO_2.

1.2.4.1 Non-metal doped TiO_2

There are three different main opinions regarding modification mechanism of TiO_2 doped with nonmetals. (1) Band gap narrowing; (2) Impurity energy levels; and (3) Oxygen vacancies.

1. Band gap narrowing: Asashi, *et al.* (2001) found N 2p state hybrids with O 2p states in anatase TiO_2 doped with nitrogen because their energies are very close, and thus the band gap of N-TiO_2 is narrowed and able to absorb visible light
2. Impurity energy level: Irie, *et al.* (2003) stated that TiO_2 oxygen sites substituted by nitrogen atom form isolated impurity energy levels above the valence band. Irradiation with UV light excites electrons in both the VB and the impurity energy levels, but illumination with visible light only excites electrons in the impurity energy level.
3. Oxygen vacancies: Ihara, *et al.* (2003) concluded that oxygen-deficient sites formed in the grain boundaries are important to emerge vis-activity and nitrogen doped in part of oxygen-deficient sites are important as blocker for reoxidation.

Kabushiki Kaisha Toyota Chuo Kenkyusho is a developer of a photocatalytic material, a titanium compound Ti-O-X, exhibiting a photocatalytic action when exposed to light with a wave length in the region of ultraviolet and visible irradiation (Morikawa *et al*., 2002). Anion X is an element

selected from B, C, P, S, Cl, As, Se, Br, Sb, Te, or I, or a molecule containing at least one of these elements. Materials are prepared by at least one of a method comprising substituting anions X for some of the oxygen sites of titanium oxide crystals, a method comprising doping anions X between lattices of a titanium crystal and a method comprising doping grain boundaries of titanium oxide, or a combination of these methods. The photocatalytic materials, described in this invention, acquired a new energy level formed in a band gap of titanium oxide, which results in its increased photocatalytic activity by absorbing visible light. Thus, the photocatalyst can exhibit satisfactory photocatalytic activity even under solar or fluorescent light.

Those materials could be manufactured by the sol-gel method, chemical reaction method, treatment in plasma containing anion species X, ion implantation and RF magnetron sputtering. In the last method, substrate and titanium oxide target are set in the vacuum chamber of a RF magnetron sputtering device. Then, appropriate amounts of gas containing anions X (for example SO_2+O_2) and an inert gas (for example Ar) is introduced into the vacuum chamber to conduct sputtering. Ti-O-X film is deposited on "substrate" surface serving as support. Various materials such as SiO_2 or ceramic were proposed for the support (Morikawa *et al*., 2002). The inventors suggested, that nonmetal-doping could improve the long-term hydrophilicity compared to that of the TiO_2 film. TiO_2/Ti-O-X film deposited on various surfaces could served as defogging agent and proofing against the effects of organic substance decomposition.

The US Patent No. 2008045410 pertains to doped anatase-TiO_2 composition that exhibits enhanced photocatalytic activity (Prochazka and Spitler, 2008). From the composition point of view, this invention provides a nanosized, crystalline titanium dioxide (anatase) composition. The composition is doped with phosphorus, and the doping level is between 0.10 and 0.55 weight percent. Providing method includes: (1) spray drying of a phosphorus-doped solution of titanium oxychloride, titanium oxysulphate or aqueous solution of another titanium salt to produce an amorphous titanium dioxide solid intermediate with homogeneously distributed atoms of phosphorous through the matter; and (2) calcining the amorphous, solid intermediate at a temperature between 300 and 900°C. Phosphoric acid could be used as phosphorus precursor. The optimal doping level is 0.33 weight percent. The photocatalytic activity of the phosphorus-

doped material is at least 100 percent greater than the undoped material (Prochazka and Spitler, 2008).

Phosphorus has a limited solubility in the anatase lattice. In a calcination step, excess phosphorus is driven out from the lattice and ends up on the particle surface. Depending on the calcination temperature, titanium phosphate, titanyl phosphate, titanium pyrophosphate or their mixtures form on the particles surface. The enhanced photodegradation activity is explained by creation a thin layer on the nanoanatase particle by excess phosphorus. Low concentration of phosphorus are evenly distributed throughout the anatase crystal lattice and accordingly will not impact absorption properties of the material. At a certain phosphorus content, a monomolecular layer of titanium phosphate is formed on the particle surface and this significantly increases the adsorption of organic compounds and accelerated the photodegradation efficiency. Further, increasing phosphorus concentration induces the formation of a compact, thicker layer of titanium phosphate or pyrophosphate. The adsorption of organic compounds on the particle surfaces is concomitantly increased, but the photoactive TiO_2 core is insulated from the compounds and photoactivity is accordingly decreased (Prochazka and Spitler, 2008).

Another invention in this category, presents a sulfur doped TiO_2 having enhanced activity in the presence of visible light, the production method and use of the same (Karvinen and Lamminmaki, 2003). A sulfur-containing titanium dioxide hydrate precipitate is obtained from an acid titanium oxysulphate solution at a temperature below the boiling point of the solution, e.g. in the range from 70 to 100°C, using crystal nuclei and without addition of base. The precipitate is separated, washed and calcinated. Calcination of the hydrate precipitate is conducted in the temperature range 100 to 500°C, most preferably in the temperature range 200 to 500°C. The catalytic activity has been observed to decrease above and under this calcinations temperature range.

The next invention deals with a carbon-doped nanostructured TiO_2 material having the following characteristics: an optical band gap lower than 2.1 eV and an optical transmittance below 90%, 50% and 10% for wavelengths lower than 650 nm, 500 nm, and 400 nm, respectively. The C-TiO_2 can be obtained by thermal assembling of TiO_2 nanoparticles in the presence of a carbon

source, which is preferably a carbon-containing atmosphere such as the air. It was observed that under thermal annealing the grain growth is modest, the nanostructure is retained and the rapid diffusion of C atoms present as contaminants in the atmosphere into titania nanocrystalline lattice is highly favored.

The last invention in this section relates to titanium oxide-based photocatalysts which are activated in the visible light and of self-cleaning materials that are prepared by substituting O of pure TiO_2 with C and N. The photocatalyst has a general formula of $TiO_{2-x-\delta}C_xN_\delta$ wherein $0 < x_{+\delta} < 0.22$, $0 < x < 0.2$, and $0 < \delta < 0.02$. A preparation method comprising a formation process of thin films by using Ti and inert gas, N_2 and CO as mixed gas by reactive sputtering, and heat treating process of the formed thin film at a temperature between 450 and 550°C for 2 to 4 hours, thereby crystallizing.

1.2.4.2 Metal doped TiO_2

The visible light photoactivity of metal-doped TiO_2 can be explained by a new energy level produced in the band gap of TiO_2 by the dispersion of metal nanoparticles in the TiO_2 matrix. As shown in **Fig. 1.5** electron can be excited from the defect state to the TiO_2 conduction band by photon with energy equals $h\nu_2$. Additional benefit of transition metal doping is the improved trapping of electrons to inhibit electron-hole recombination during irradiation. Decrease of charge carriers recombination results in enhanced photoactivity.

Oxonica Ltd. is a developer of innovative surface-doped particles of TiO_2 and ZnO. Their invention relates to metal-doped nanoparticles, which find utility as stabilizing ingredients within cosmetics to prevent degradation from sun light, for use in agriculture, horticulture and veterinary medicine, as coatings for plastics and for environmental protection. A particles of TiO_2 or ZnO were doped with one or more other elements such as concentration of dopant in the surface of the particle is greater than that at the core of the particles. Suitable dopants for the oxide particles include manganese (especially in the form of Mn^{3+}), vanadium, chromium, cerium, selenium, iron, nickel, copper, tin, aluminum, lead, silver, zirconium, zinc and cobalt. The surface-doped particles of the present invention can be obtained by combining particles of a

host lattice (TiO_2) with a second component in the form of a salt in solution in water, and then baking it, typically at a temperature of at least 300°C and then calcining it at a higher temperature, for example at least 500 or 600°C.

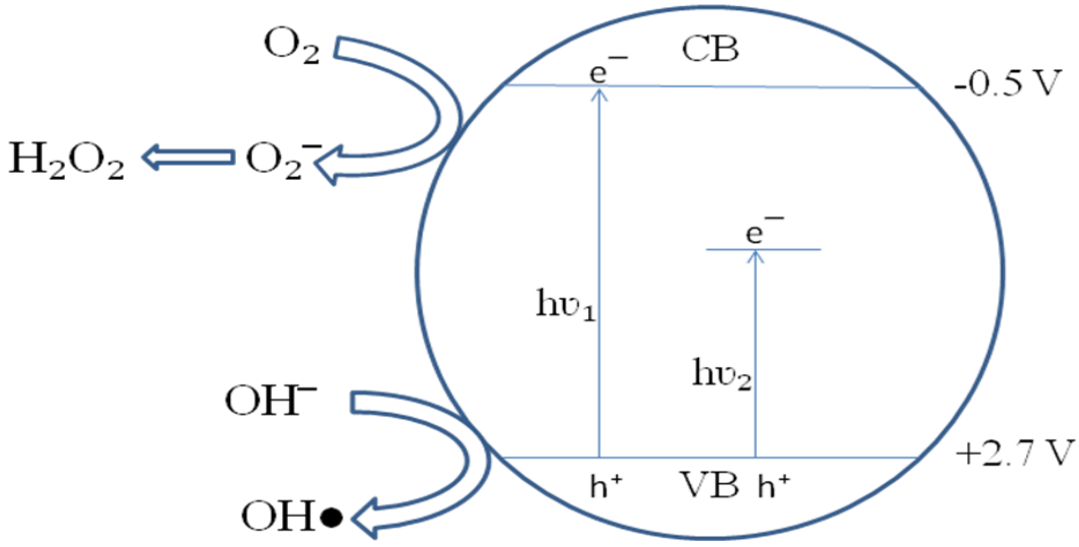

Fig. 1.5 Mechanism of photocatalysis of metal deposited TiO_2 using LI method under UV light irradiation (Zaleska, 2008)

Patent application, published in 2006, is related to a method for preparing TiO_2/SiO_2 aerogel micro-ball doped with iron. Iron-doped TiO_2 could be obtained by mixing $TiOSO_4$ and $FeCl_3$ with deionized water and adjusting pH value to 7-8. Obtained precipitate is washed and mixed with nitric acid solution at 50-90°C. Subsequently, silica sol is prepared by mixing of silica sol with nitric acid and anhydrate ethyl alcohol. Then, titanium sol is mixed with SiO_2 alcohol sol at 1:3-8 volume ratio. TiO_2/SiO_2 composite sol is added into oil phase to obtain micro ball, washed with acetone and dried. Obtained micro-balls have diameter from 10 to 200 μm. Described method represents a low-cost and simple process for doped-nanoparticles manufacturing.

Another invention is related to TiO_2 doped with molybdenum (Mo) (Arai and Sasazawa, 1988). TiO-Mo monocrystalline substance could be obtained by mixing TiO_2 with MoO_3 in the specific proportion, pressure molding the mixture and calcining this in air. The above-mentioned molded body of TiO_2 doped with Mo consists of polycrystalline substance well-regulated in crystal size.

In case of the proportion of Mo doped in single crystal is less than 2.0 mol%, the granular growth of crystal is not caused but it is made dense and intercrystalline cracking is not caused. In case the proportion of Mo is more than 8.0 mol%, the granular growth of crystal is irregularly caused and the intercrystalline cracking is not caused.

US6884739 is related to lanthanide-doped TiO_x dielectric films obtained by plasma oxidation (Ahn and Forbes, 2005). A method of forming a dielectric film includes evaporating a Ti source at a first rate to deposit a Ti on a substrate, evaporating a lanthanide source at a second rate to form a lanthanide doped Ti film, and oxidize the Ti/lanthanide film to grow a dielectric film on a substrate. The Ti and the lanthanide are evaporated using electron beam evaporation or are assisted by ion beam bombardment of the substrate surface during deposition. The evaporation of the Ti and lanthanide is followed by oxidation using a Kr/oxygen plasma.

The next invention provides pyrogenically prepared titanium dioxide doped by an aerosol and containing, as a doping component, an oxide selected from the group consisting of zinc oxide, platinum oxide, magnesium oxide and/or aluminum oxide as the doping components (Hemme *et al*., 2006) Invented photocatalyst has either: a) a BET surface area of 65 m^2/g to 80 m^2/g and a doping component concentration of 40 ppm to 800 ppm, or b) a BET surface area of 35 m^2/g to 60 m^2/g and a doping component concentration of more than 1000 ppm.

Japanese patent application describes method for crystallizing metal-doped TiO_2 thin film and laminate having metal-doped TiO_2 thin film (Shino *et al.*, 2007). In this method, a polymer film is subjected to a plasma treatment by applying high frequency electric power between two electrodes in an argon gas atmosphere, thereby the metal-doped TiO_2 thin film highly crystallized and with enhanced electroconductivity is obtained.

Another invention refers to metallic ion-doped nano TiO_2 transparent photocatalytic emulsion and preparation method thereof (Ding, 2007). According to the invention optical transparent lotion features in 0.5 to 10% TiO_2 mixed with V, Sn, Zn, Fe, 1 to 10% emulsifier with the rest being water. It is obtained by making of titanic chloride water solution containing metal ions is hydrolyzed to generate TiO_2, VO_3 and Sn^{4+}, Zn^{2+}, Fe^{3+} or Ce^{3+} compound oxidation deposit. This

method uses cheap titanium tetrachloride and ammonium vanadate, iron trichloride, tin tetrachloride and zinc sulfate, using low temperature complex hydrolysis to allow higher ability to mix and expanding spectral response zone to visible light. Photocatalytic emulsion could be used for the degradation of organic pollutants utilizing sun light or irradiation emitted by fluorescent lamps (Ding, 2007).

REFERENCES

1. Ahn, K.Y. and Forbes, L. (2005): US20056884739.
2. Anjaneyulu, Y., Chary, N. S., and Raj, D. S. S. (2005). Decolourization of industrial effluents- available methods and emerging technologies. *Rev. Environ. Sci. Biotechnol*, 4, 245–273
3. Anpo M. (1997). Preparation of Ti-HMS mesoporous materials and their photocatalytic reactivity for the decomposition of NO into N_2 and O_2. *Catal. Surv. Jpn.*, 1, 169
4. Anpo M. (2000), In Studies in Surface Science and Catalysis, 130, The 12th International Congress on Catalysis *(Elsevier),* Part A, *157*
5. Al-Bastaki N.M. (2003). Treatment of synthetic industrial waste-water with UV/TiO_2 and RO using benzene as a model hydrocarbon, *Desalination*, 156, 193.
6. Al-Sayyed G., D'Oliveira J.C., and Pichat P. (1991). Semiconductor-sensitized photodegradtion of 4-chlorophenol in water. *Photochem. Photobiol. A* 58 , 99.
7. Arai, K. and Sasazawa, K. (1998): JP63050324.
8. Asahi R, Morikawa T, Ohwaki T, Aoki K. and Taga Y (2001). Visible-light photocatalysis in nitrogen-doped titanium dioxide. *Science*, 293, 269-271.
9. Behnajady M.A., Modirshahla N., Shokri M., and Rad B. (2008). Enhancement of photocatalytic activity of TiO_2 nanoparticles by silver doping : Photodepostion versus Liquid Impregnation methods. *Global Nest*., 10, 1-7
10. Behnajady M.A., Moghaddam S.G., Modirshahla N., and Shokri M. (2009). Investigation of the effect of heat attachment method parameters at photocatalytic activity of immobilized ZnO nanoparticles on glass plate. *Desalination*, 249, 1371–1376
11. Bussi, J., Ohanian, M., Vazquez, M., and Dalchiele, E.A. (2002). Photocatalytic Removal of Hg from solid wastes of chlor-Alkali Plant. *Environ. Eng.*, 128 (8), 733.
12. Chakrabarti S. and Dutta B.K. (2004). Photocatalytic degradation of model textiles dyes in waste-water using ZnO as semiconductor catalyst. *Hazard Mater.*, 112,269–278.
13. Chatterjee D. and Dasgupta S. (2005). Visible light induced photocatalytic degradation of organic pollutants. *Photochem Photobiol C – Photochem Rev* 6, 186–205.
14. Cruz AM-dl, Mart´ınez D.S. and Cu´ ellar E.L. (2010) Synthesis and characterization of WO3 nanoparticles prepared by the precipitation method: evaluation of photocatalytic activity under vis-irradiation. *Solid State Sci.*, **12**, 88–94.

15. Ding J., Sun S., Bao J., Luo Z., and Gao C. (2009). Synthesis of $CaIn_2O_4$ rods and its photocatalytic performance under visible-light irradiation. *Catal Lett.,* 130, 147–153.
16. Ding, S.L. (2007): CN101062476.
17. El-Bahy Z.M., Ismail A.A., and Mohamed R.M. (2009). Enhancement of titania doping rare earth for photogeneration of organic dye (Direct Blue). *Hazard Mater.,* 166,138–143.
18. Fijishima A. and Honda K. (1972). Electochemical photolysis of water at a semiconductor electride. *Nature*, 238, 37.
19. Galvez J.B. and Rodríguez S.M. (2003) Solar Detoxification, Edition de l'UNESCO.
20. Gan, L.T. (2007): CN1966141.
21. Gao Y., Chen B., Li H., and Ma Y. (2003). Preparation and characterisation of a magnetically separated photocatalyst and its catalytic properties. *Mater Chem Phys.,* 80:348–355.
22. Ghasemi S., Rahimnejad S., Setayesh S.R., Rohani S., and Golami M.R. (2009). Transistionmetal ions effect on the properties and photocatalytic activity of nanocrystalline TiO2 prepared in an ionic liquid. *Hazard Mater*, 172, 1573–1578
23. Goren Z., Willner I., Nelson A.J. and Frank A.J. (1990). Selective photodegradation of CO_2/HCO_3^- to formate by aqeous suspensions and colloids of Pd-TiO_2 *Phys. Chem.*, 94 , 3784.
24. Grassian V.H. (2005). Environmental catalysis, 1^{ST} Ed. Taylor &Francis.
25. Guin D, Manorama S V, Latha J N L and Singh S. (2007). Photoreduction of silver on bare and colloidal TiO_2 nanoparticles/nanotubes: Synthesis, characterization, and tested for antibacterial outcome. *Phys. Chem*. C, 111 **,** 13393
26. Guo Y., Yang X., Ma F., Li K., Xu L., and Yuan X. (2010). Addictive-free controllable fabrication of bismuth vanadates and their photocatalytic activity toward dye degradation. *Appl Surf Sci.,* 256, 2215–2222
27. Han .F, Kambala V.S.R., Srinivasan M., Rajarathnam D. and Naidu R. (2009). Tailored titanium dioxide photocatalyst for the degradation of organic dyes inwaste-water treatment: a review. *Appl Catal A– Gen.,* 359.25–40
28. Hatch, K.L., and Maibach, H.I. (1995). Textile dermatitis: An update. (I). Resins, additives and fibers. *Contact Dermatitis,* 32, 319–326.
29. Hemme, I., Mangold, H., Geissen, S.U., Moiseev, A. (2006): US20066992042.

30. Hern´andez-Alonso M.D., Fresno F., Su´arez S., and Coronado J.M. (2009). Development of alternative photocatalysts to TiO_2: challenges and opportunities. *Energy Environ Sci*, 2, 1231–1257.
31. Herrmann J.M., Disdier J., Pichat P., Fernandez A., Gonzalez Elipe A., Munuera G. and Leclercq C.(1991). Titania supported catalyst synthesis by photocatalytic codeposition at ambient temperature: preparation and characterization of Pt-Rh, Ag-Rh and Pt-Pd couples. *Catal*., 132, 490.
32. Hoffmann M.R., Martin S.T., Choi W. and Bahnemann D.W. (1994) Environmental Applications of Semiconductor Photocatalysis, *Chem. Rev*., 95(1), 69.
33. Hunger, K. (2005). Toxicology and toxicological testing of colorants. *Rev. Prog. Color.*, 35, 76–89.
34. Ihara T., Miyoshi M., Triyama Y., Marsumato O. and Sugihara S. (2003). Visible-light-active titanium oxide photocatalyst realized by an oxygen-deficient structure and by nitrogen doping. *Appl Catal B*, 42, 403-409.
35. Irie H., Watanabe Y. and Hashimoto K. (2003). Nitrogen-concentration dependence on photocatalytic activity of $TiO_{2-x}N_x$ powders. *Phys Chem B*, 5483-5486.
36. Janitabar-Darzi S. and Mahjoub A.R. (2009). Investigation of phase transformation and photocatalytic properties of sol-gel prepare nanostructured ZnO/TiO2 composites. *Alloys Compd.*, 486, 805–808
37. Janus M., Choina J., and Morawski A.W. (2009). Azo dyes decomposition on new nitrogen-modified anatase TiO_2 with high adsorptivity. *Hazard Mater.*, 166, 1–5 .
38. Kansal S.K., Singh M. and Sud D. (2007). Studies on photodegradation of two commercial dyes in aqueous phase using different photocatalysts. *Hazard Mater.*, 141, 581–590.
39. Karvinen S., Lamminmaki R.J. (2003): WO03082743.
40. Linsebigler, A.L., Lu G., and Yates J.T. (1995). Photocatalysis on TiO_2 surfaces: Principles, Mechanisms, and Selected Results. *Chem. Rev*., 95, 735.
41. Longstaff, E. (1983). An assessment and categorization of the animal carcinogenicity data on selected dyestuffs and an extrapolation of those data to an evaluation of the relative carcinogenic risk to man. *Dyes Pigments,* 4, 243.

42. Lu C., Wu Y., Mai F., Chung W., Wu C. and Lin W. (2009). Degradation efficiencies and mechanisms of the ZnO-mediated photocatalytic degradation of Basic Blue 11 under visible light irradiation. *Mol Catal A – Chem.,* 310, 159–165.
43. Lv Y., Yu L., Huang H., Liu H., and Feng Y. (2009). Preparation, characterization of P-doped TiO2 nanoparticles and their excellent photocatalystic properties under the solar light irradiation. *Alloy Compd.,* 488, 314–319.
44. Mai F.D., Chen C.C., Chen J.L. and Liu S.C. (2008) Photodegradation of methyl green using visible irradiation in ZnO suspensions. Determination of the reaction pathway and identification of intermediates by a HPLC-photodiode array-electrospray ionisation-mass spectrometry method. *Chromatogr A,* **1189**, 355–365.
45. Morikawa T., Asahi R., Ohwaki, T. and Taga, Y. (2002): EP1205245A1
46. Muruganandham M., Swaminathan M. (2007). Solar driven decoulorisation of Reactive Yellow 14 by advanced oxidation processes in heterogeneous and homogeneous media, *Dyes and Pigments,* 72, 137.
47. Nah Y.C., Paramasivam I., and Schmuki P. (2010). Doped TiO_2 and TiO_2 nanotubes: synthesis and applications. *Chem Phys Chem* , 11, 2698 – 2713
48. Naoi K, Ohko Y and Tatsuma T (2004). TiO_2 films loaded with silver nanoparticles: control of photochromic behavior. *Am. Chem. Soc*. 126**,** 3664
49. Nishio J., Tokumura M., Znad H.T. and Kawase Y. (2006). Photocatalytic decolorisation of azo-dyewith zinc oxide powder in an externalUV light irradiation slurry photoreactor. *Hazard Mater.,* 138,106–115.
50. Ohko Y, Tatsuma T, Fujii T, Naoi K, Niwa C, Kubota Y and Fujishima A. (2003). Multicolor photchromism of TiO_2 films loaded with silver nanoparticles. *Nat. Mater*. 2**,** 29
51. Ohno T., Mitsui T., and Matsumura M. (2003). Photocatalytic activity of S doped TiO_2 photocatalyst under visible light. *Chem. Lett.*, 32, 364.
52. Øllgaard, H., Frost, L., Galster, J., and Hansen, O.C. (1998). Survey of azocolorants in Denmark: Consumption, use, health and environmental aspects, No. XX1998 Ministry of Environment and Energy, Denmark, Danish Environmental Protection Agency, November

53. Pozzo R.L., Baltan´as M.A., and Cassano A.E. (1997) Supported titanium dioxide as photocatalyst in water decontamination: state of the art. *Catal Today* , 39, 219–231.
54. Pare B., Jonnalagadda S.B., Tomar H., Singh P., and Bhagwat V.W. (2008). ZnO assisted photocatalytic degradation of acridine orange in aqueous solution using visible irradiation. *Desalination* 232, 80–90.
55. Peavy H.S., Rowe D.R., Tchobanoglous G. (1985). Environmental Engineering, McGraw-Hill.
56. Pinheiro, H. M., Touraud, E., and Thomas, O. (2004). Aromatic amines from azo dye reduction: Status review with emphasis on direct UV spectrophotometric detection in textile industry wastewaters. *Dyes Pigments,* 61, 121–139.
57. Prochazka J. and Spitler T. (2008): US2008045410.
58. Qiu R., Zhang D., Mo Y., Song L., Brewer E., and Huang X. (2007). Photocatalytic activity of polymer-modified ZnO under visible light irradiation. *Hazard Mater.,* 156, 80–85 .
59. Rauf M.A and Ashraf S.S. (2009), Radiation induced degradation of dyes – an overview. *Hazard Mater.,* 166,6–16.
60. Sahoo C., Gupta A.K. and Pal A. (2005). Photocatalytic degradation of Crystal Violet (C.I. Basic Violet 3) on silver ion doped TiO2, *Dyes Pigments*, 66, 189-196.
61. Sakkas V.A., Islam M.A., Stalikas C., and Albanis T.A. (2010). Photocatalytic degradation using design of experiments: a review and example of the congo red degradation. *HazardMater* ,175, 33–44.
62. Saien J., Asgari M., Soleymani A.R. and Taghavinia N. (2009). Photocatalytic decomposition of direct red 16 and kinetics analysis in a conic body packed bed reactor with nanostructure titania coated Raschig rings. *Chem Eng,* 151, 295–301.
63. Shang M., Wang W., Zhou L., Sun S. and Yin W. (2009). Nanosized $BiVO_4$ with high visible-light induced photocatalytic activity: ultrasonicassisted synthesis and protective effect of surfactant. *Hazard Mater*., 172, 338–344.
64. Shino, O., Iwabuchi, Y. and Ono, S. (2007): JP07039270.
65. Sobana N., Muruganadham M. and Swaminathan M. (2006). Nano-Ag particles doped TiO_2 for efficient photodegradation of Direct azo dyes, *Mol. Catal. A*, 258, 124-132.

66. Szabó-Bárdos E., Czili H. and Horváth A. (2003). Photocatalytic oxidation of oxalic acid enhanced by silver deposition on a TiO2 surface, *Photochem. Photobiol. A*, 154, 195-201.
67. Tang J., Zou Z., Katagiri M., Kako T. and Ye J. (2004).Photo catalytic degradation of MB on MIn2O4 (M=akali earth metal) under visible light: effects of crystal and electronic structure on the photocatalytic activity. *Catal Today*, **93–95**, 885–889.
68. Tethis S.R.L., Barborini E., Milani P. and Piseri P.G.C. (2006): WO06002916.
69. Turchi C.S. and Ollis D.F. (1990). Photocatalytic degradation of organic water contaminants: mechanisms involving hydroxyl radical attack. *Catal*. 122 ,178
70. UNESCO (2002). Is the World on Track.
71. UNICEF (2002) The State of the World's Children.
72. Uygur, A. (1997). An overview of oxidative and photooxidative decolorisation treatments of textile wastewaters. *JSDC*, 113, 211–217
73. Vamathevan V., Amal R., Beydoun D., Low G. and McEvoy S. (2002). Photocatalytic oxidation of organics in water using pure and silver-modified titanium dioxide particles, *Photochem. Photobiol. A*, 148, 233-245.
74. Viana B.C., Ferreira O.P., Filho A.G.S., Rodrigues C.M., Moraes S.G., Filho J.M. *et al*. (2009). Decorating titanate nanotubes with CeO2 nanoparticles, *Phys Chem C*, 113, 20234–20239.
75. Wade J. (2005). M.Sc. Thesis, An Investigation of TiO_2-$ZnFe_2O_4$ Nanocomposites for Visible Light Photocatalysis, University of South California, 2005**.**
76. Wakefield, G., Park, B.G., Lipscomb, S. and Holland, E. (2006): WO05072680.
77. World Health Organisation, Reducing Risks, Promoting Healthy Life, 2002
78. Yamashita H., Harada M., Misaka J., Takeuchi M., Ikeue K., and Anpo M. (2002), Preparation of efficient titanium oxide photocatalysts by an ionized cluster beam method and their application for the degradation of propanol diluted in water. *Photochem. Photobiol.* A , 148, 257.
79. Yin W., Wang W., Zhou L., Sun S., and Zhang L. (2010). CTAB-assisted synthesis of monoclinic $BiVO_4$ photocatalyst and its highly efficient degradation of organic dye under visible-light irradiation. *Hazard Mater*, 173, 194–199.

80. Yu J.C., Ho W., Yu J., Yip H.P., Wong P.K., and Zhao J. (2005). Efficient visible light induced photocatalytic disinfection on sulfur –doped nanocrystalline titania. *Environ. Sci. Technol*, 39, 1175
81. Zhang S. and Song L. (2009). Preparation of visible-light-active carbon and nitrogen codoped titanium dioxide photocatalyst with the assistance of aniline. *Catal Commun.* ,10, 1725–1729.
82. Zheng R., Guo Y., Jin C., Xie J., Zhu Y. and Xie Y. (2010), Novel thermally stable phosphorous-doped TiO_2 photocatalyst synthesized by hydrolysis of $TiCl_4$. *MolCatal A–Chem*, 319, 46–51.
83. Zhu J., Xie J., Chen M., Jiang D., and Wu D. (2010). Low temperature synthesis of anatase rare earth doped titania-silica photocatalyst and its photocatalytic activity under solar-light. *Colloids Surf A Physicochem Eng Asp* ,355, 178–182.
84. Znad H. and Kawase Y. (2009). Synthesis and characterisation of S-Doped Degussa P-25 with application in decolorization of Orange II as a model substrate. *Mol Catal A – Chem.*, 314, 55–62

CHAPTER 2

MATERIALS AND METHODS

This section describes the materials as well as the methods used to conduct the experimental work

2.1 MATERIALS

2.1.1 Chemicals and reagents

All chemicals used were of A.R. grade. These were purchased from Sigma-Aldrich chemicals PVT. Ltd. India, SD Fine and Merck, India. All chemicals were used as received in all experiments and distilled water was used.

The chemicals used were $AgNO_3$ (Qualigens Fine Chemicals), 1N HCl and 1N NaOH for adjusting pH, buffer solutions (pH=7 and pH=4) for caliberating pH meter.

2.1.2 Effluents

Reactive black 5 dye (55% dye content) was procured from Sigma Aldrich. Reactive black 5 is diazo dye with λ_{max} 597 nm. The structure of RB 5 is shown in **Fig. 2.1**.

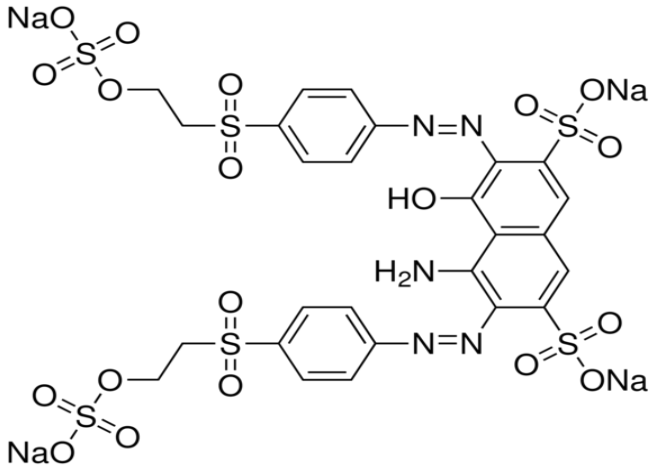

Fig. 2.1. Structure of Reactive Black 5

2.1.3 Catalyst

The catalyst used was Degussa P25 Aeroxide TiO_2 procured from Degussa Company, Germany. Its physiochemical properties are given in **Table 2.1.**

Table 2.1: Physiochemical properties of Degussa P25 TiO_2

Physical state	White powder
Composition (%)	≈80% anatase, ≈20% rutile
Density (g/cm^{-3})	3.8
BET surface area (m^2/g)	≈55
Average particle size (nm)	≈30
pH in aqueous solution	3-4

2.1.4 Instruments/Equipment

2.1.4.1 Radiometer

UV intensity inside the reactor was measured by Eppley radiometer (model no. 33013)

2.1.4.2 pH meter

The pH of the solution was measured using ELICO, India, model no. LI 120 pH meter.

2.1.4.3 UV-Vis spectrophotometer

The concentration of the compounds was determined via spectroscopic analysis. A double beam spectrophotometer from Electronic Corporation India limited (ECIL), model UV 5704 SS was used.

2.1.4.4 Centrifuge

Samples were centrifuged after treatment in order to separate the TiO_2 particles from the solution. A compact laboratory centrifuge Hitachi High-Speed Micro Centrifuge, Model CF15RX II was used. Samples were centrifuged at a speed of 14,500 RPM until the solution appeared completely free of TiO_2 particles.

2.1.4.5 Photoreactor

The set up consisted of a batch reactor (Toor, 2005) placed on a platform under UV lamps housed in a lamp box (**Fig. 2.2 and Fig. 2.3**). The lamp box (4'x 2.5' x 2.5') used was made up of galvanized aluminium sheet and fitted with 8 UV black tubes of 40 W each, fitted in parallel on the top of reactor. The UV lamps emit radiation in the range of 300-400 nm, with the peak intensity at 350 nm. UV intensity for all experiments was kept at 10 W/m².

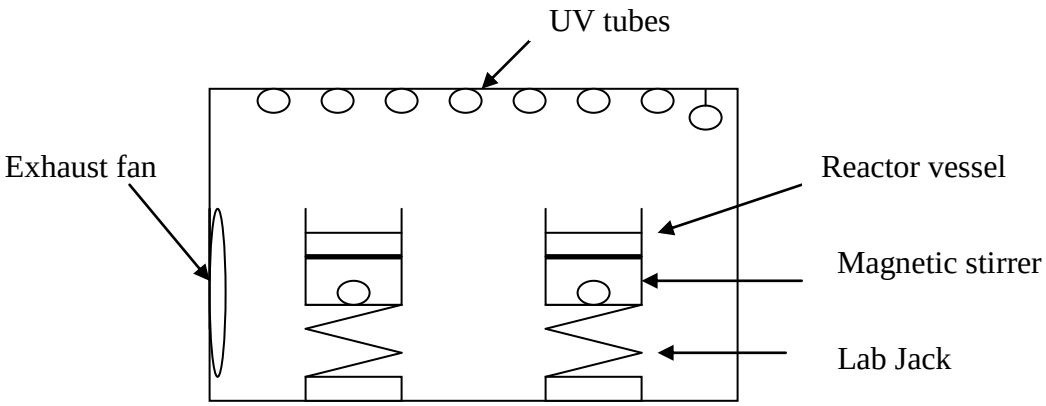

Fig. 2.2. Scheme of the photocatalytic reactor

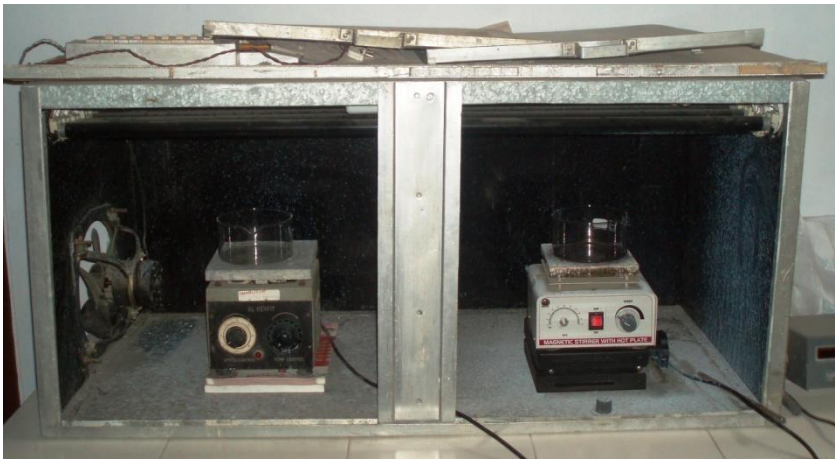

Fig. 2.3. Photograph of the photocatalytic reactor set up

An exhaust fan is located on the side of the box, allow to keep a constant temperature inside the reactor as well as ensuring a sufficient amount of O_2 in the air.

2.2 EXPERIMENTAL PROCEDURE

2.2.1 Method for preparation of silver doped TiO_2

Doped TiO_2 was prepared by Liquid Impregnation method (LI) which consisted of following steps:

First 5 g of TiO_2 was added in 100 ml distilled water. Then to this TiO_2 suspension, silver nitrate in various percentages was added, in which silver concentration was 0.5, 1.0, 1.5 and 2.5 % (mole ratio) versus TiO_2. The slurry was stirred well and allowed to rest for 24 hrs and dried in oven at 100 °C for 12 hrs. the dried solids were grounded into pieces in agate mortar and calcined in muffle furnace at 400 °C for 5 hrs (Sahoo *et al*., 2005).

2.2.2 Adsorption on TiO_2 suspension

The adsorption characteristics of RB5 on to TiO_2 (doped and undoped) surface were studied by exposing 100 mg/l of dye solution to different amounts of catalyst (doped and undoped TiO_2). The dye solution was mixed vigorously in a stirrer with catalyst for 30 minutes. The samples were withdrawn and centrifuged to determine the absorbance at 597 nm to estimate the dye concentration in the supernatant for adsorption.

2.2.3 Photocatalytic treatment

A Borosil circular glass vessel of 500 ml capacity was used as photocatalytic reactor. The area to volume ratio (A/V) of the reactor was kept at 0.202 cm^2/ml for all experiment. This reactor is placed on the lab jack so that required UV intensity could be attained by adjusting the distance of the vessel from the UV tubes. A magnetic stirrer was used to keep the reactor contents well mixed, so that the TiO_2 (doped and undoped) stayed suspended. The samples were withdrawn from reactor and centrifuged at 14,500 rpm for 15 minutes to separate catalyst particles.

2.3 ANALYTICAL PROCEDURES

2.3.1 Determination of Reactive black 5 concentration using UV-Vis spectrophotometer

A PC based UV-Vis spectrophotometer was used for determination of the concentration of the synthetic effluent following the given below procedure

- The system was switched on and warmed up
- Thoroughly clean cuvettes were used
- Both of the cuvettes were filled with distilled water to get the reference base line
- One cuvette was then emptied and filled with the solution for which the concentration was to be measured; the other cuvette stays as a reference
- The spectrum was recorded (typically the analysis was done between 200 to 600nm)
- The absorbance value at 597 nm was used to calculate the concentration being the λ_{max} for this dye.
- The relationship between the concentration and the absorbance value is given by the Beer-Lambert law (Williams and Flemming, 2005; Atkins, 2002). A calibration curve was made using standard solution of RB 5 of known concentration. The concentration range for the calibration curve was 50 to 100 mg/l.

A linear fit of the curve Absorbance = f (concentration) was made and the equation was used to calculate the concentration from the absorbance value obtained.

REFERENCES

1. Atkins P. (2002) Physical Chemistry, Oxford University Press, 7th edition.
2. Sahoo C., Gupta A.K. and Pal A. (2005). Photocatalytic degradation of Crystal Violet (C.I. Basic Violet 3) on silver ion doped TiO2, *Dyes Pigments*, 66, 189-196.
3. Toor A.P. (2005). PhD. Thesis, Photocatalytic degradation of chlorinated organic compounds in industrial wastewater, Thapar University, Patiala, India.
4. Williams D.H. and Fleming I. (2005), Spectroscopic Method in Organic Chemistry, Tata-Mc Graw Hill, 5th edition.

CHAPTER 3

KINETICS OF ADSORPTION AND OF PHOTOCATALYTIC DEGRADATION OF RB 5 CATALYSED BY TiO_2 PHOTOCATALYST

3.1 KINETICS OF ADSORPTION

The adsorption phenomenon depends upon the contact time between the dye solution and adsorbent. In the case of physical adsorption, most of the adorbate species are adsorbed within short interval of contact time. However, in the case of chemical adsorption, adsorbent requires a longer contact time for the attainment of equilibrium. Adsorption phenomenon is fast during the initial stages and becomes slower near the equilibrium. During the initial stage, large number of active sites are available hence adsorption is more. After certain interval of time, the remaining vacant surface sites are difficult to be occupied due to repulsive forces between the solute molecules on the solid and bulk phases. The effect of contact time under different catalyst load on the absorption of RB 5 (0.5 g/l -3.0 g/l) for 100 mg/l dye concentration at pH=2 onto the TiO_2 surface is shown in the **Fig. 3.1**. RB 5 showed faster rate of adsorption during first 5 mins of dye-TiO_2 contact time.

The initial concentration provides an important driving force to overcome all mass transfer resistances of all molecules between the aqueous and solid phases. The equilibrium was reached within 10 min. After this equilibrium period, the amount of adsorbed dye did not show time-dependent change.

For bare TiO_2 the kinetic adsorption data were processed to study the dynamics of the adsorption process in terms of the order of rate constant Values of the rate constant (k_1), equilibrium adsorption capacity (q_e), the correlation coefficient (r^2) were calculated from the plots of $\log(q_e - q_t)$ versus t (for pseudo-first-order reaction) and t/q_t versus t (for pseudo-second-order reaction) for each catalyst load (0.5 g/l-3.0 g/l) as represented in Table 3.1.

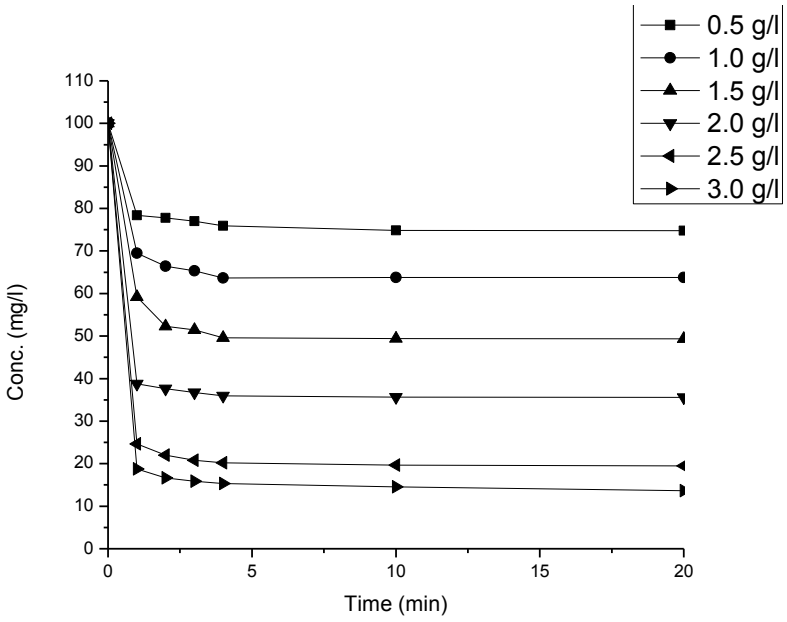

Fig. 3.1. Adsorption studies of RB 5 on bare TiO_2 (Dye conc. = 100 mg/l, pH=2) at different TiO_2 concentration

The calculated q_e values for pseudo-first-order model do not agree with the experimental values. The plots of t/q_t versus t showed a linear relationship with r^2=0.99 to1 for pseudo-second-order kinetics model. The calculated q_e values agree very well with the experimental data and this indicates that the adsorption of dye on TiO_2 surface follows a pseudo-second-order kinetics model.

3.2 ADSORPTION ISOTHERMS

The analysis of adsorption process requires a study of equilibrium adsorption. The equilibrium adsorption test provides the physico-chemical data on the applicability of the adsorption for bare TiO_2. **Fig. 3.2** gives the adsorption isotherm at pH=2.

Table3.1: Adsorption kinetic parameters for different catalyst loadings (0.5 g/l-3.0 g/l) for 100 mg/l dye concentration at pH=2

	First-order kinetic model				Second-order kinetic model		
Catalyst load (g/l)	q_e(exp.) (mg/g)	k_1(1/min)	q_e (calculated) (mg/g)	r^2	k_2 (g/mg.min)	q_e (calculated) (mg/g)	r^2
0.5	50.45	0.41	11.68	0.8762	0.014	50.50	0.99
1.0	36.32	0.622	10.36	0.97	0.203	36.60	0.99
1.5	33.96	0.622	12.1	0.81	0.262	34.01	0.99
2.0	32.16				0.662	32.20	1
2.5	32.18				0.6	32.26	1
3.0	28.92				0.3	28.98	0.99

Adsorption test was carried in the absence of light to insure that no photocatalytic reaction takes place. The adsorption experiments were conducted with 100 mg/l dye concentration at pH=2 at different catalyst concentrations (0.5 g/l-3.0 g/l). The data were fitted using the Langmuir and Freundlich models. The Langmuir model is applicable to homogeneous adsorption systems when there is no interaction between sorbate molecules, while the Freundlich model is an empirical equation used to describe heterogeneous systems and is not restricted to the formation of the monolayer.

A plot between C_e/q_e and C_e is shown in **Fig. 3.3** shows a good fit with r^2 value of 0.9947 and the value of K_L comes out as 0.21294 l/g. The value of dimensionless separation (R_L) (Eq.(16)) is 0.0448. The value of R_L between zero and one indicates the favorable shape of Langmuir isotherm.

The linearized equation that describes the Freundlich isotherm is given by Eq. (18), where K_F is the adsorption capacity (mg/g) and 1/n is the adsorption intensity (l/g).

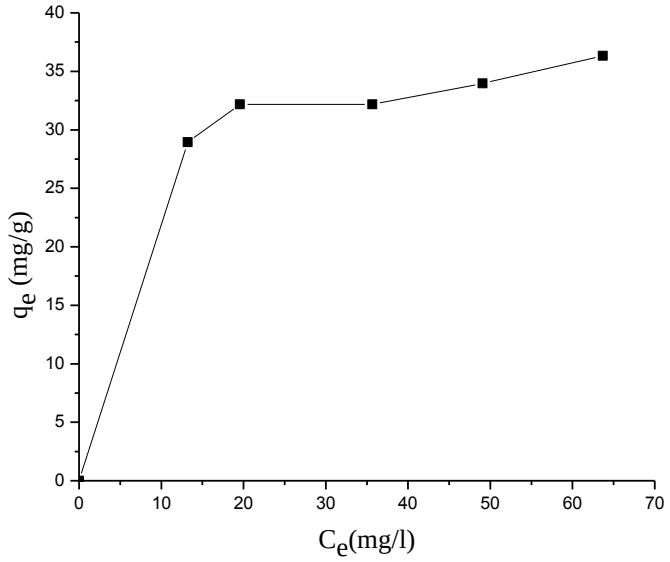

Fig. 3.2. Adsorption isotherm of RB 5 onto bare TiO_2 surface (Dye conc. = 100 mg/l, pH=2)

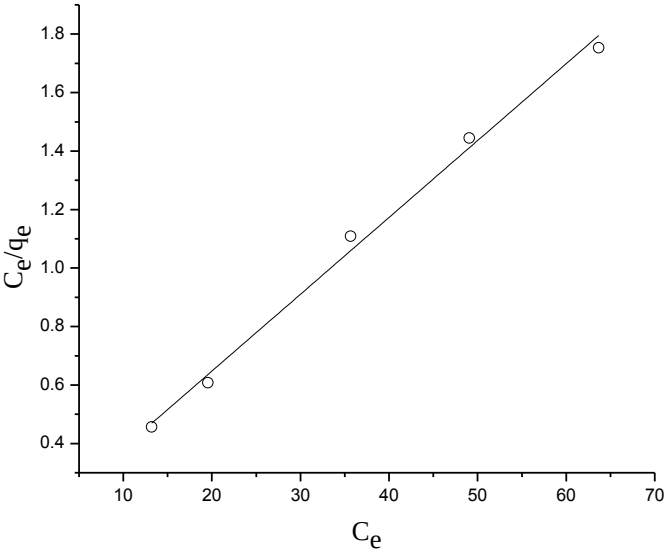

Fig. 3.3. Langmuir adsorption isotherm of RB 5 onto bare TiO_2 surface (Dye conc. = 100 mg/l, pH=2)

Through the plot between log Q_e and log C_e (**Fig. 3.4**), the values that fit the experimental data were K_F = 20.12 L/g, 1/n = 7.3 with a correlation coefficient value (r^2) = 0.9612

The r^2 value of both Langmuir and Freundlich isotherms show that both the models are well suited to fit the adsorption isotherm data. **Table 3.2** shows the values of q_{mon}, K_L, R_L for Langmuir isotherms and K_F, n for Freundlich isotherms for reactive black 5.

3.3 THERMODYNAMIC PARAMETERS

The values of ΔGº indicate that the adsorption process is non-spontaneous at lower catalyst load (0.5 g/l-2.0 g/l). The value of ΔGº is negative for 2.5 g/l and 3.0 g/l catalyst load indicating spontaneous adsorption process at these values of catalyst load as shown in Table 3.3.

.

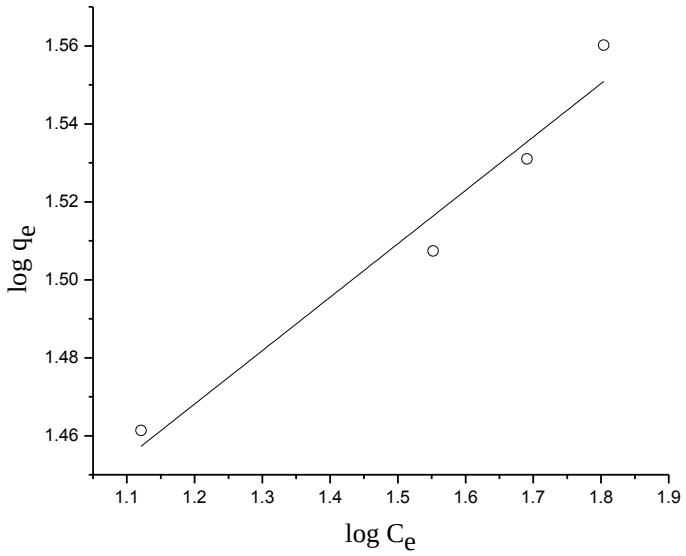

Fig. 3.4. Freundlich adsorption isotherm of RB 5 onto bared TiO_2 surface (Dye conc. = 100 mg/l, pH=2)

Table 3.2: Langmuir and Freundlich isotherm for adsorption of reactive black 5 on TiO_2 surface (Dye conc. =100 mg/l, pH=2)

Langmuir Isotherm	Reactive black 5	
	q_{mon} (mg/g)	38.46
	K_L (L/mg)	0.21
	R_L	0.0448
	r^2	0.99
Freundlich Isotherm	K_F (L/g)	20.12
	N	7.3
	r^2	0.96

Table 3.3: Thermodynamic parameters of the adsorption of RB 5 on TiO_2 surface (Dye conc. =100 mg/l, pH=2)

Cat load (g/l)	K (l/g)	ΔGº (kJ/ mol)
0.5	0.674758	0.974
1.0	0.570449	1.390
1.5	0.692322	0.911
2.0	0.901775	0.256
2.5	1.645829	-1.234
3.0	2.189855	-1.942

3.4 PHOTOCATALYTIC DEGRADATION STUDIES

$$r = -\frac{dC}{dt} = kK_{ads}C = k'C \quad (21)$$

where *k*' is the apparent rate constant of the pseudo-first order kinetics. The integral form, *C*= *f*(*t*) of the rate equation is:

$$ln\frac{C}{C_O} = -k't \quad (22)$$

where C_O is the initial concentration of reactive black 5 dye.

Fig. 3.5 shows the photocatalytic activity of TiO_2. After adsorption in dark for 30 min (200 mg/l dye concentration, catalyst load 2.5 g/l and pH=2) the dye adsorbed was near about 85 mg/l. The residual dye concentration in the solution was then irradiated with UV for 6 hr.

After photocatalytic treatment for 6 hr, the dye concentration left was 14 mg/l i.e. 87 % degradation occurred.

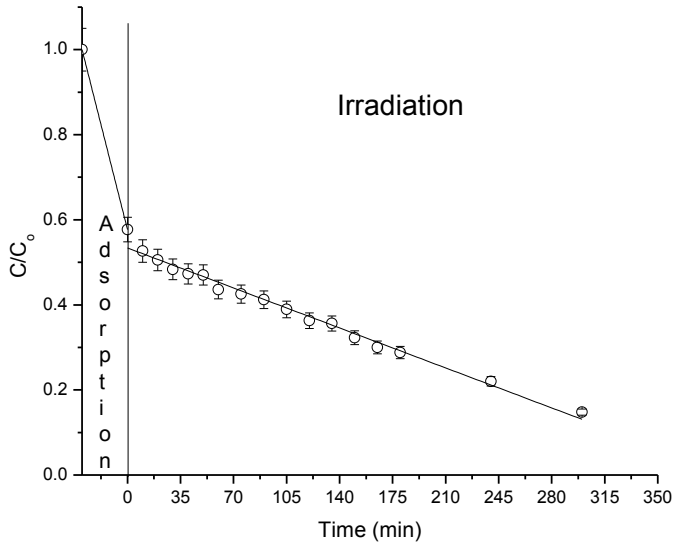

Fig . 3.5. Photodegradation of reactive black 5 on bared TiO_2 surface. (Dye conc. = 200 mg/l, cat load= 2.5 g/l, pH=2**)**

From Eq. (20) the value of K_{ads} is calculated by plotting graph between $1/k_{app}$ and C. For bared TiO_2 (**Fig. 3.6**) comes out to be 0.159 l/mg and value of k is 2.99 mg/l-min. The value of $K_{ads}C$ in the denominator cannot be neglected with respect to unity. The photocatalytic oxidation rate approaches first order

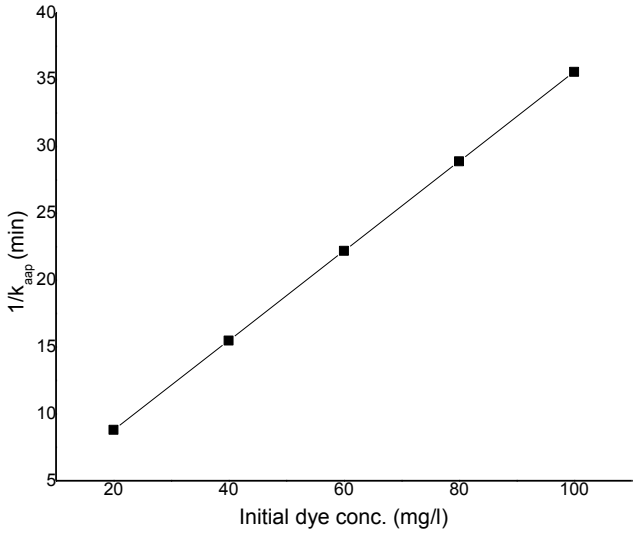

Fig. 3.6. Langmuir-Hinshelwood model graph for bare TiO_2

CHAPTER 4

KINETICS OF ADSORPTION AND OF PHOTOCATALYTIC DEGRADATION OF RB 5 CATALYSED BY SILVER DOPED TiO_2 PHOTOCATALYST

4.1 KINETICS OF ADSORPTION

The effect of contact time under different catalyst (silver doped TiO_2) loadings on the adsorption of RB 5 (0.5 g/l -3.0 g/l) for 100 mg/l dye concentration at pH=2 onto the TiO_2 surface is shown in the **Fig. 4.1**.

For silver doped TiO_2, the dye solution (100 mg/l) at solution pH=2 did not undergo any observable adsorption on to the photocatalyst surface on stirring in the dark for 40 min. The dye absorbed was 95 mg/l.

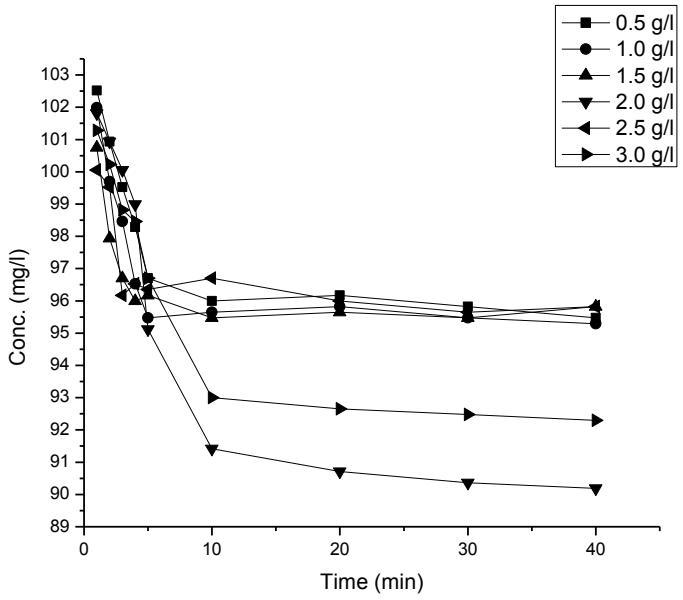

Fig. 4.1. Adsorption studies of RB 5 by silver doped TiO_2 (Dye conc. = 100 mg/l, pH=2)

4.2 PHOTOCATALYTIC DEGRADATION STUDIES

For silver doped TiO_2 the photocatalytic degradation was examined both at pH=2 and at solution pH=5.7. The degradation at solution pH (=5.7) was better than at pH=2. Poor adsorption in dark means that for silver doped TiO_2 catalyst value of K_{ads} can't be calculated.

Fig. 4.2 shows the photocatalytic activity of silver doped TiO_2. After adsorption in dark for 30 min (200 mg/l dye concentration, catalyst load 2.5 g/l and pH=5.7) the dye adsorbed was near about 195 mg/l. The residual dye concentration in the solution was then irradiated with UV for 3 hr.

After photocatalytic treatment for 6 hr, the dye concentration left was 10 mg/l i.e. 95 % degradation occurred.

4.2.1 Effect of silver doping

Photocatalytic degradation of RB 5 in the presence of silver doped TiO_2 follows the pseudo first order reaction as shown in **Fig. 4.3**. The graph between ln (C/C_o) versus irradiation time for 100 mg/l dye concentration and catalyst load 2 g/l for undoped TiO_2 and 2.5 % doped TiO_2 is a straight line which shows the reaction follows pseudo first order reaction (**Fig. 4.3**).

The silver doping method is more efficient than undoped TiO_2 at decolorization of RB 5. TiO_2 in the presence of UV light generates electrons and holes which trigger the further radical reaction. Electrons and holes can recombine which reduces the rate of photo catalytic degradation. Silver doping reduces the recombination of electrons and holes (Coleman *et al.*, 2005). Electrons are trapped by oxygen adsorbed on the photo catalytic surface to form superoxide radical (Daneshvar *et al*., 2004) and holes on the surface of TiO_2 oxidize adsorbed water or hydroxyl ions to form hydroxyl radicals.

In liquid impregnation method the silver is deposited as Ag^+ ions. These ions consume electrons and get reduced to metallic silver. Hence e^--h^+ recombination is reduced (Vamathevan *et al.*, 2002). Electron trap by Ag^+ ion to get reduced to metallic silver is more efficient as compared to

trapping by oxygen molecule to form superoxide radical (Szabo-Bardos *et al*., 2003). Hence metallic silver is produced at faster rate as compared to superoxide radical and therefore formation of O_2● is less.

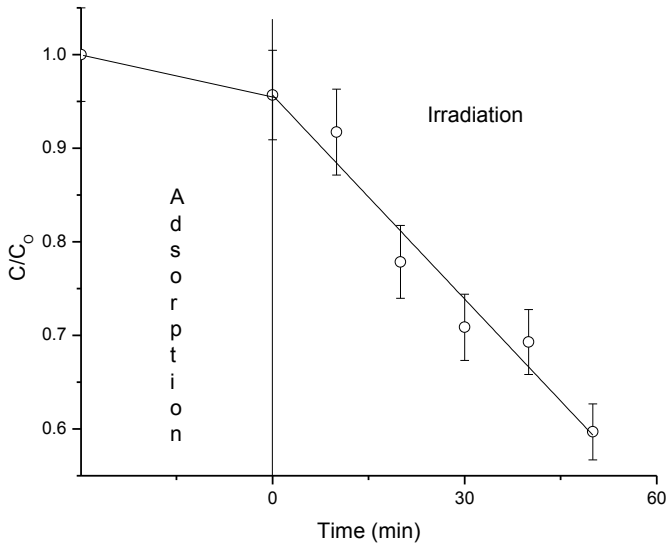

Fig. 4.2. Photodegradation of reactive black 5 on silver doped TiO_2 surface. (Dye conc. = 200 mg/l, cat load= 2.5 g/l, pH=5.7).

4.2.2 Effect of doping level

Effect of percentage doping on degradation of dye is shown in **Fig. 4.4**. As shown in figure, the value of apparent constant increases with the increase in percent doping.

At low value of percentage doping (0.5%) the value of k_{aap} is less than the value for undoped TiO_2 which increases with the increase in percentage doping, reaches at some maximum value and then again decreases. Results in **Fig. 4.4** shows that the optimum value of silver loading for the decolorization of reactive black 5 is 2.5%. At high value of percentage doping the excessive amount of silver loading on TiO_2 decreases the amount of light reaching on to the surface of TiO_2, thus less number of electrons and holes are generated and hence reducing the

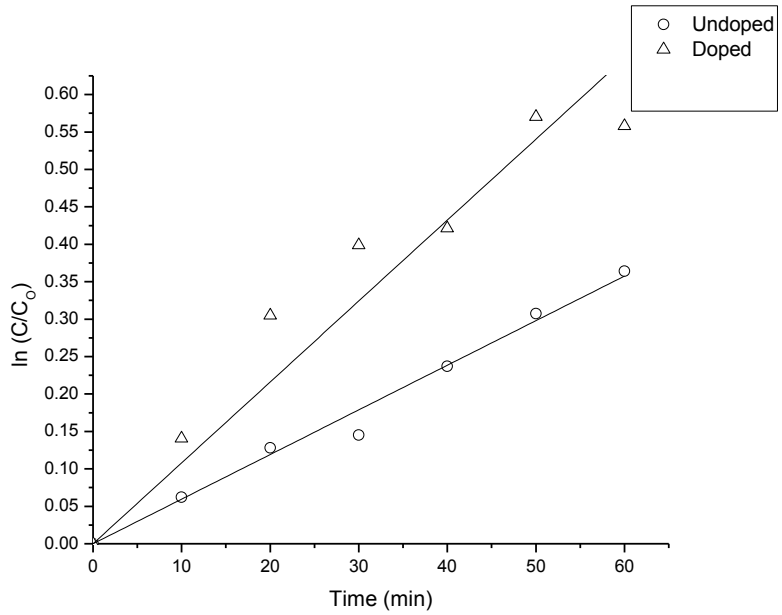

Fig. 4.3. Effect of dye concentration of doped and undoped TiO_2 at the degradation of RB 5 (dye conc. =100 mg/l, catalyst load= 2.5 g/l and 2.5 % doping).

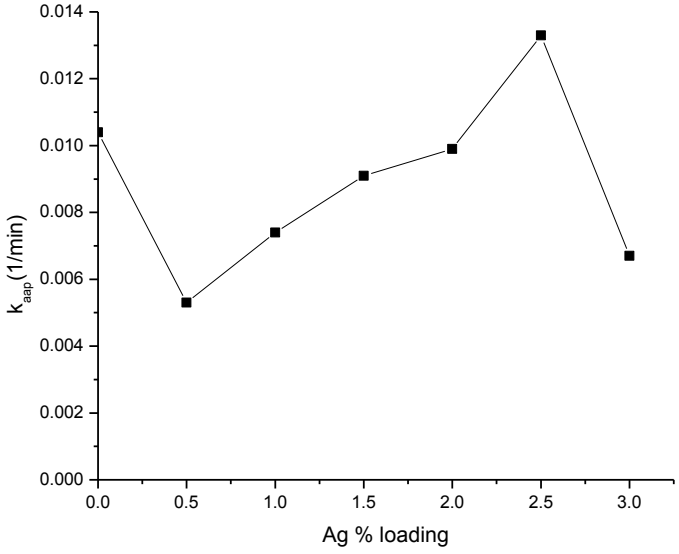

Fig. 4.4. Effect of silver content on the photocatalytic activity of TiO_2 at the degradation of RB 5

photocatalytic activity of TiO_2. Moreover, the active sites on TiO_2 surface can be occupied by silver particles for the desired photocatalytic reactions leading to the reduction in activity of TiO_2 (Coleman *et al*., 2005). The probability of the hole capture is increased by the large number of silver particles at high silver loadings, which decrease the probability of holes reacting with adsorbed species at the TiO_2 surface (Sobana *et al*., 2006).

REFERENCES

1. Coleman H.M., Chiang K. and Amal R. (2005). Effects of Ag and Pt on photocatalytic degradation of endocrine disrupting chemicals in water, *Chem. Eng.*, **113**, 65-72.
2. Daneshvar N., Rabbani M., Modirshahla N. and Behnajady M.A. (2004). Kinetic modeling of photocatalytic degradation of Acid Red 27 in UV/TiO2 process, *Photochem. Photobiol. A*, **168**, 39-45
3. Sobana N., Muruganadham M. and Swaminathan M. (2006). Nano-Ag particles doped TiO_2 for efficient photodegradation of Direct azo dyes, *Mol. Catal. A*, **258**, 124-132.
4. Szabó-Bárdos E., Czili H. and Horváth A. (2003). Photocatalytic oxidation of oxalic acid enhanced by silver deposition on a TiO_2 surface, *Photochem. Photobiol. A*, **154**, 195-201.
5. Vamathevan V., Amal R., Beydoun D., Low G. and McEvoy S. (2002) Photocatalytic oxidation of organics in water using pure and silver-modified titanium dioxide particles, *Photochem. Photobiol. A*, 148, 233-245.

CHAPTER 5
CONCLUSIONS

Anatase form of TiO_2 can efficiently photocatalyse the degradation of reactive black 5 using artificial UV light. Optimum degradation parameters (catalyst load, pH, dye concentration etc) should be obtained to achieve high degradation rate.

In this work, the kinetics of adorption and photocatalytic degradation of RB 5 using undoped and silver doped TiO_2 has been shown.

The adsorption kinetics of undoped TiO_2 shows that it follows pseudo-second-order kinetics. The adsorption phenomenon depends upon the contact time between the dye solution and adsorbent. Langmuir and Freundlich isotherms show that both the models are well suited to fit the adsorption isotherm data. However, silver doped TiO_2 showed poor adsorption results.

Silver doped TiO_2 showed pronounced effect on degradation under UV light as compared to bare TiO_2. Under UV irradiation the photocatalytic degradation of RB 5 was achieved up to 99% in 6 hr using silver doped TiO_2 as compared to 87% in 6 hr in undoped TiO_2

Silver doped TiO_2 is more efficient than undoped TiO_2 for photocatalytic degradation of RB 5. The positive effect of silver on the photoactivity of TiO_2 for degradation of RB 5 may be explained by its ability to trap electrons. This process reduces the recombination of light generated electron-hole pairs at TiO_2 surface. Silver content has an optimum value of 2.5% in LI for achieving high photocatalytic activity.

5.1 RECOMMENDATIONS AND FUTURE WORK

The future works on photocatalytic treatment could go towards analyzing the effect of other parameters such as: the UV intensity, the influence of O_2, the influence of metallic ions in the solution, the geometry of the reactor and finally the addition of electron acceptor such as H_2O_2 without using an univariate method.

The analysis of the TiO_2 particle (doped and undoped) at the end of the treatment should be conducted and research should be done to find ways to recover the catalyst at the end of the photocatalytic treatment.

It would also be interesting to design an outdoor reactor and implement its installation in India to confirm the possibility of the sun as the source of energy to activate the catalyst in this treatment.

Finally, an economical study of the process as part of an effluent treatment plant is necessary if one want to enhance such process in the industry.